Islamic University of Gaza

High Studies Deanery

Faculty of Engineering

Master in Science

Civil Engineering

Soil Pressure Behind Retaining Wall with Narrow Backfill

دراسة تأثير ضغط التربة الجانبي من الردم المحدود على الحائط الاستنادي

Submitted By
Ayman M. Nassar

Supervised By
Dr. Jihad Hamad

A thesis submitted in partial fulfillment of the requirement for Degree of Master of Science in Civil Engineering

January, 2012

بسم الله الرحمن الرحيم

{يَرْفعِ اللَّه الذَّين آمنَوُا منِكْم واَلذَّينِ أُوتوُا العْلِم دَرجَات واَللَّه بِما تعَمْلوُنَ خَبيِر}

المجادلة الآية 11

صدق الله العظيم

DEDICATION

I would like to dedicate this work to my family specially my mother who supports me in all stages of my life and to my loving caring wife, for their sacrifice and endless support.

ACKNOWLEDGMENT

First of all, all thanks and appreciations go to Allah for His unlimited blessings and for giving me the strength to complete this study

I would like to extend my sincere appreciation and special thanks to my supervisor **Dr. Jihad Hamad**, for his guidance, patience and encouragement.

I deeply thank **Dr.Abed Al-Majid Nassar** for his infinite support and encouragement. Also, I want to express my love and gratitude to my loving family for their encouragement and support.

Additionally, I would like to extend my acknowledgement to my colleagues for their support. I forward my special thanks to **Engr. Amr Abu Al-Qmbz, Engr. Hussien Hussien, Engr. Adel Abdallah** and **Engr. Adel Babaa** for their support and encouragement.

Finally, I would like to thank all the staff of the Material and Soil Laboratory at the Islamic University of Gaza especially **Engr. Ahmed Al-Kurd, Engr. Adel Hamad and Mr. Tahseen Shihada** who have supported and encouraged me to accomplish this work. Also, special thanks to **Engr. Mohammed Swalha** from the Material and Soil Laboratory in the Engineering Syndicate for his superior help.

Abstract

High traffic demands have led to widening of existing highways to accommodate increased traffic volume. However, due to the high cost of widening the roads and limited space available at the site, construction of earth retaining walls is often done under a constrained space. This leads to retaining walls with narrow backfill. This type of walls is referred as "Narrow" retaining walls. Various studies suggest the mechanics of narrow retaining walls differs from traditional walls and the lateral earth pressures in narrow retaining walls are no longer properly predicated by using conventional at-rest or active equations. This research presents the study of retaining wall in case of narrow backfill. Both of theoretical study and experimental work were conducted to calculate the effect of soil pressure at different backfill width ratios. Theoretical study was carried out using numerical analysis (plaxis software program). Different cases were simulated at different aspect ratio (w/H) ranging between 0.2 to 1.4 by 0.2 increment. In addition, the experimental work was performed to verify the obtained results by numerical modeling. The experimental work was conducted using a centrifugal model and Geo-kon device was employed to measure the soil pressure.

The results indicated that, due to boundary constraint, the earth pressure decreases as the decrease of the wall aspect ratio also, the results show that lateral earth pressure coefficient considerably becomes constant at aspect ratio of 0.6 and less than rankine earth pressure coefficient at active condition. This implies that earth pressure theories would overestimate the earth pressures and the design based on the values of conventional earth pressure is somewhat overly conservative and uneconomical when applying to the design of narrow walls. Accordingly, different charts were developed due to experimental work and theoretical study to calculate the lateral earth pressure for narrow backfill.

ملخص البحث

زيادة حركة المرور أدت الى توسيع الطرق لاستيعاب الزيادة في حجم المرور، ورغم التكلفة الإضافية لتوسيع الطريق ، الا أنه في الغالب يتم بناء الجدران الإستنادية رغم ضيق المسافة. و يسمى هذا النوع من الجدران الإستنادية " بالجدران الإستنادية محدودة الردم" . وقد اثبتت الدراسات السابقة ان الأحمال على هذا النوع من الجدران يختلف عن الطرق التقليدية المعتمدة (at-rest and active condition) في حساب الاحمال الافقية.

خلال هذا البحث فقد تم دراسة تأثير التربة الجانبي في حالة الردم الضيق (narrow backfill at active condition) ، و لقد تمت الدراسة بناء على العمل التجريبي و على الدراسة النظرية باستخدام النموذج الرياضي (برنامج plaxis) حيث تم نمذجة الردم الجانبي على ابعاد مختلفة (w/H) تتراوح ما بين 0.2 و 1.4 بتزايد منتظم و قيمته 0.2. و قد تم القيام أيضا بالعمل التجريبي من خلال نموذج فيزيائي و تم استخدام جهاز Geo-kon لقياس ضغط التربة.

و لقد اشارت نتائج هذا البحث أن ضغط التربة الجانبي يقل كلما نقص عرض الردم المحدود خلف الجدار الإستنادي، حيث يصبح معامل التربة الجانبي ثابت على الأغلب بعد القيمة (w/H=0.6) وهي أقل من قيمة معامل (Rankine coefficient) . وهذا يثبت أن استخدام الطرق التقليدية في حساب الاحمال الواقعة على الحائط الاستنادي في حالة الردم المحدود مبالغ فيها وغير اقتصادية، لذلك فقد تم عمل العديد من العلاقات التي توضح العلاقة بين عرض الردم و معامل الضغط الجانبي في حالة (at active condition).

TABLE OF CONTENTS

LIST OF FIGURES

LIST OF TABLES

LIST of SYMBOLS

k_c:	Calculated Lateral Earth Pressure Coefficient.
k_r:	Rankine Lateral Earth Pressure Coefficient at Active Condition.
$k_{a(coulomb)}$	Coulomb Lateral Earth Pressure Coefficient at Active Condition.
P_a:	Lateral Active Force.
γ:	Soil Unit Weight.
$\emptyset$:	Soil Friction Angle.
σ_a:	Active lateral Earth Pressure.
w:	Backfill Width.
H:	Height of Retaining Wall.
w/H:	Backfill Width Ratio.
FE:	Finite Element
E:	Young's Modulus.
ϑ:	Poisson's Ratio.
c:	Soil Cohesion.
φ:	Dilatancy Angle.

Chapter 1
Introduction

Retaining wall is a type of engineering structure which is used to withstand lateral forces exerted by soil retained or surcharge and maintained the difference between elevations of ground surface. Type of wall to be used is very much depends on site condition (Wahab, 2008).

The forces imposed on the wall need to be assessed and taken into consideration. These forces are not a unique property of the soil, but it is a function of the loads that the soil behind the structure must carry and the groundwater condition. The pressure exerted by the soil on these structures is known as earth pressure and must be determined before a satisfactory design can be made. Moreover, there are many theories were developed to calculate the lateral earth pressure on retaining wall. Rankine and Coulomb theories are the most common used to calculate the lateral earth pressure on retaining wall.

This research will focus on calculating and measuring the active earth pressure behind retaining wall with narrow backfill. This type of retaining walls structure was raised due to traffic demand which leads to widen of existing highways to accommodate the traffic volume increasing. As the population increases and development of urban areas becomes a priority, the traffic demands have increased which has led to widening of existing highways to accommodate increased traffic volume. However, due to the high cost of widening the road and limited space available at site, construction of earth retaining walls is often done under a constrained space. (Yang & Liu, 2007).

To describe the pressure soil will exert, a lateral earth pressure coefficient, k, is used. k is the ratio of lateral earth pressure to vertical pressure ($k = \sigma_h'/\sigma_v'$). Thus, horizontal earth pressure is assumed to be directly proportional to the vertical pressure at any given point in the soil profile. k can depend on the soil properties. Lateral earth pressure coefficients are broken up into three categories: at-rest, active, and passive. There are many theories

for predicting lateral earth pressure; some are empirically based, and others are analytically determined.

1.1 Problem statement

Almost design of retaining wall structures is based on Coulomb's or Rankine's theory to calculate the lateral earth pressure. These theories were developed to describe the pressure on retaining wall in case of unlimited backfill. In this research, the study focused on the effect of soil pressure on retaining wall with narrow backfill (*the backfill is constrained*).

1.2 Scope of work

The main scope of this research is to study the effect of soil pressure on retaining wall in case of narrow backfill (limited width)

Main Objectives:

- Determine the coefficient of lateral earth pressure (k) through experimental work and theoretical study.
- Develop charts show the relation between the backfill width ratio (w/H) and the lateral earth pressure coefficient.
- Develop charts show the relation between the depth ratio (d/H) and lateral earth pressure coefficient.
- A comparison between the obtained results from experimental testing and theoretical study.
- A comparison with others studies.

1.3 Methodology

The research was started by reviewing all previous studies related to this project, and then these were summarized in a good way to present the results. After that, theoretical study was adopted using numerical modeling (plaxis software program). Additionally, experimental work was conducted to verify the results obtained by numerical modeling. The experimental work was implemented using a centrifugal model besides and a Geo-kon device was used to measure the soil pressure.

1.4 Thesis Structure

The chapters in this thesis are arranged carefully in the order or sequence of steps to make it clear and understandable. Five chapters are presented in this research. ***Chapter one*** is an introductory chapter which provides detailed information about the nature of this study. It discusses the research problem; it also contains the research goals, objectives and the outline methodology.

Chapters two is oriented as a literature review about the main topic of this study: "Soil Pressure on Behind Retaining Wall with Narrow Backfill " referring to the previous studies performed on this subject.

Chapter three explains and describes the methodology of research. The methodology is introduced with details to include the theoretical study and the experimental work.

Chapter four highlights the results and discussion of both theoretical study and experimental work. In addition, relation between these results was taken into consideration through this chapter.

Finally, ***chapter five*** summarizes the main findings and conclusions of this research as well as the suggested recommendations.

Chapter 2
Literature Review

This chapter presents the review of works that were performed to determine the pressure developed against retaining walls with emphasis on retaining wall with constrained backfill behind the wall as shown in Figure 2.1. This review yielded information from laboratory tests and numerical analysis. Most of the laboratory experimental results have focused on horizontal earth pressures against at-rest walls and provide insight the effect of wall aspect ratio on horizontal earth pressure coefficients. In addition, the literature presents the theoretical work using numerical analysis especially plaxis software program. Meanwhile, studies employing limit equilibrium analysis were also reviewed. Limit equilibrium analyses have been used to calculate earth pressure coefficients and produce design charts to calculate the horizontal earth pressures.

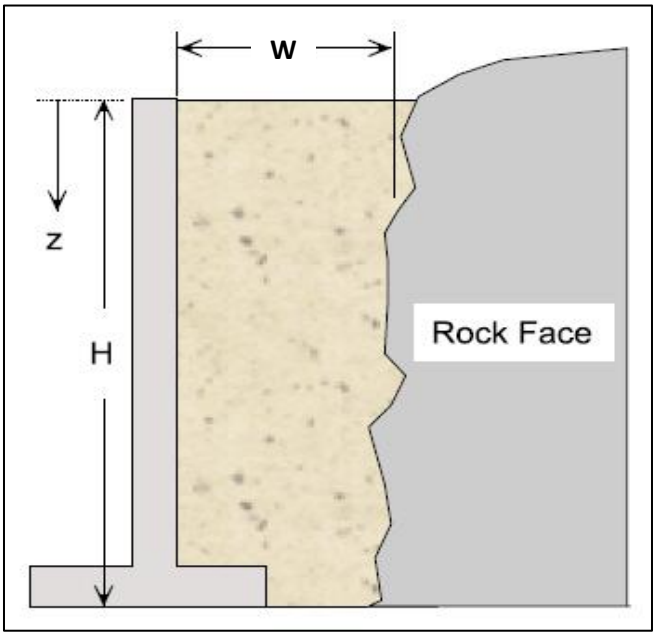

Figure 2.1: Narrow retaining wall (Yang & Liu, 2007).

2.1 Lateral Earth Pressures

Lateral earth pressure problems are highly importance and of great interest in geotechnical engineering. In many earth retaining problems, it is necessary to study the exact distribution of the earth pressure behind the retaining wall. Many researchers have studied this distribution (Motta, 1994).

Knowledge of lateral earth pressures is very crucial to design the retaining wall. The lateral earth pressures are the pressures developed by the backfill retained by the wall. Several soil parameters should be known by the designer in order to assess the wall design and its overall stability. These parameters are:

- Soil friction angle.
- Soil unit weight.
- Water table location.
- Soil cohesion.

The theoretical formulations of Coulomb's (1776) and Rankine's (1857) theories are still the fundamental approaches to the analysis of majority of retaining walls types. These conventional design methods as well as other ones, assume that adequate lateral displacement will occur to create fully active condition behind the retaining wall. (Goh, 1993).

2.1.1 Coulomb's Theory

Coulomb's theory (1776) is one of the earliest methods for computing earth pressures against walls. The main assumptions of this theory, among others that soil should be isotropic; homogeneous; has internal friction and cohesion; the rupture surface is a plane surface; the friction resistance is uniformly distributed along the rupture surface and there is a wall friction (Bowel, 1988).

To apply Coulomb's active earth pressure theory. Consider a retaining wall with its back face inclined at an angle β with the horizontal as shown in Figure 2.2. The

backfill is a granular soil that slopes at an angle α with the horizontal and δ' is the angle of friction between the soil and the wall (i.e. the angle of wall friction).

Under active pressure, the wall will move away from the soil mass. The failure assumed to be plane failure such as BC1, BC2 …etc. So to find the active force, consider a possible soil failure wedge ABC1. The forces acting on this wedge (per unit length at right angles to cross section in Figure 2.2 are as follows (Das, 2011).

- The weight of the wedge, W
- The resultant, R, of the normal and resisting shear forces acting along the failure surface BC1.
- The force R will be inclined at an angle ϕ' to the normal drawn to BC1
- The active force per unit length of the wall. P_a, which will be inclined at angle δ' to the normal drawn to the back face of the wall

For the equilibrium purposes, a force triangle can be drawn as shown in Figure 2.2. Note that θ_1 is the angle that the failure plane BC_1 makes with the horizontal. Because the magnitude of W, as well as the directions of all three forces is known, the value of the active force P_a can now be determined. Similarly, the active forces of other trial wedges, such as ABC_2, ABC_3… can be determined. The maximum value of P_a thus can be determined, which may be expressed as

$$P_a = \frac{1}{2} k_a \gamma H^2$$

Where; k_a : Coulomb's active pressure coefficient.

$$k_a = \frac{\sin^2(\beta + \phi')}{\sin^2 \beta \sin(\beta - \delta') \left[1 + \sqrt{\frac{\sin(\phi' - \delta')\sin(\phi' - \alpha)}{\sin(\beta - \delta')\sin(\alpha + \beta)}}\right]^2}$$

And H : height of the wall

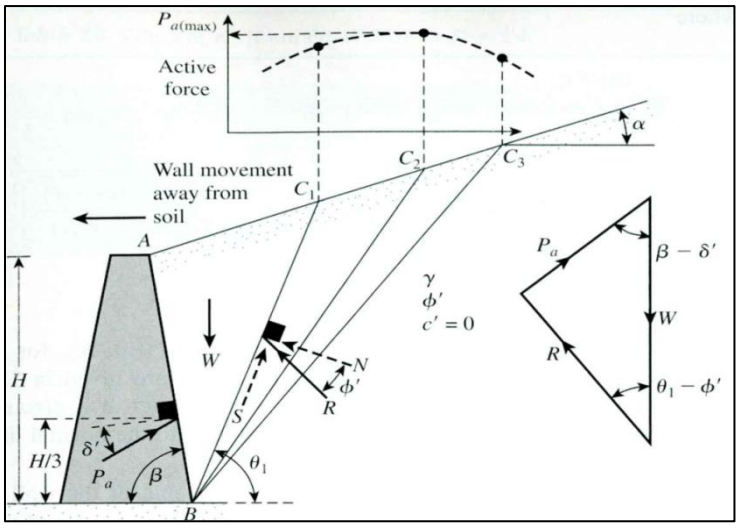

Figure 2.2: Coulomb's active earth pressure theory

2.1.2 Rankine Theory

Rankine's theory (1857) considered the soil in an equilibrium state and used the same assumptions as Coulomb except that he assumed no wall friction or soil cohesion. Rankine also used a plane failure as shown in Figure 2.3. He used Mohr circle to represent the state of stress at failure in a two- dimensional element as shown in Figure 2.4. The angle of internal friction ϕ and cohesion c, as denoted in Figure 2.4, are the relevant shear strength parameters. The shear failure occurs along a plane at angle of (45+ ϕ/2) to the horizontal plane as shown in Figure 2.3. In the case that the whole soil mass is stressed such that the stresses at each point are in the same directions then, theoretically, there will be a network of failure planes, known as a slip line field, equally inclined to the horizontal planes as shown in Figure 2.3 (Bowel, 1988).

In case of large horizontal displacement of the wall Δx, Mohr-Coulomb failure envelop defined by the following equation;

$$s = c' + \sigma' \tan\varphi$$

From Figure 2.4, it is shown that the principle stresses for Mohr's circle that touches the Mohr-Coulomb failure envelop.

$$\sigma_1^{'} = \sigma_3^{'} = \tan^2\left(45 + \frac{\phi^{'}}{2}\right) + 2c^{'}\tan\left(45 + \frac{\phi^{'}}{2}\right)$$

Mohr' circle in Figure 2.4 shows the major principal stress $\sigma_1^{'} = \sigma_0^{'}$ and the Minor principal stress $\sigma_3^{'} = \sigma_a^{'}$, thus

$$\sigma_0^{'} = \sigma_a^{'}\tan^2\left(45 + \frac{\phi^{'}}{2}\right) + 2c^{'}\tan\left(45 + \frac{\phi^{'}}{2}\right)$$

$$\sigma_a^{'} = \frac{\sigma_0^{'}}{\tan^2\left(45 + \frac{\phi^{'}}{2}\right)} - \frac{2c^{'}}{\tan\left(45 + \frac{\phi^{'}}{2}\right)}$$

$$\sigma_a^{'} = \sigma_0^{'}\tan^2\left(45 - \frac{\phi^{'}}{2}\right) - 2c^{'}\tan\left(45 - \frac{\phi^{'}}{2}\right)$$

$$= \sigma_0^{'}k_a - 2c^{'}\sqrt{K_a}$$

Where k_a is the active soil pressure coefficient: $k_a = \tan^2\left(45 - \frac{\phi^{'}}{2}\right)$.

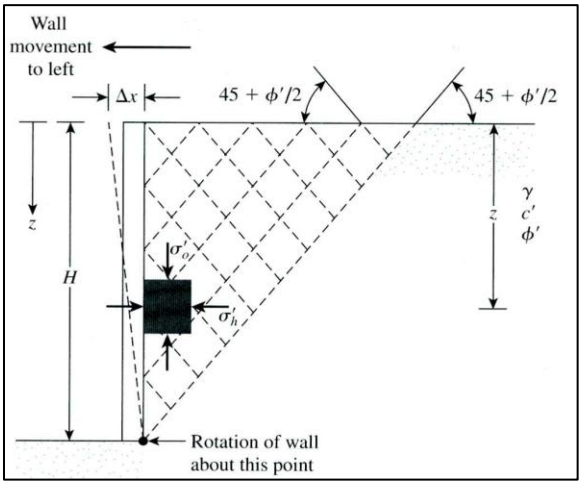

Figure 2.3: Rankine's active pressure (Das, 2011**).**

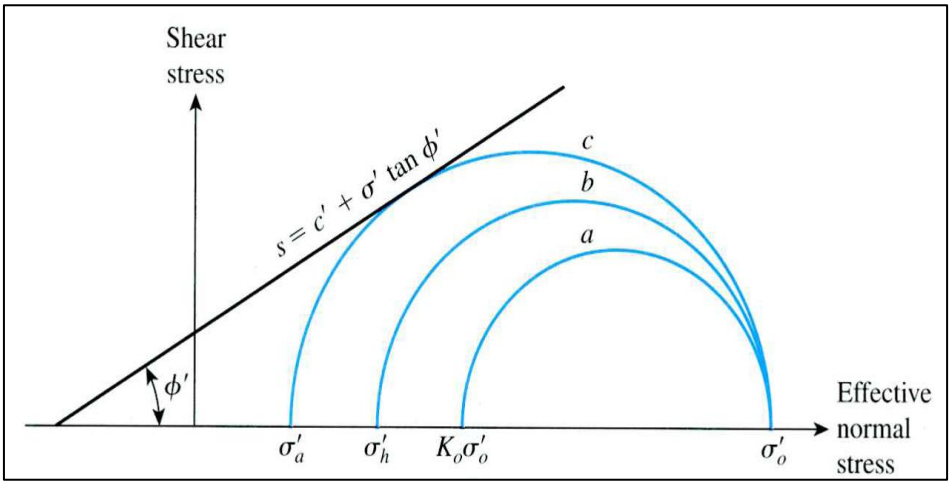

Figure 2.4: Rankine's active pressure - Mohr Circles (Das, 2011**).**

2.2 Narrow retaining walls theories

Study of soil pressure against retaining wall in case of constrained backfill is considered highly important and of a great interested to the geotechnical engineering. Accordingly, there are several studies were conducted to describe the soil pressure for limited backfill. Actually, the lateral earth pressure could be categorized into three types based on wall displacement which are rest, active and passive conditions. Previous studies took into consideration the lateral earth pressure at rest condition.

Other studies used different methods to show the effect of soil pressure on retaining wall namely, laboratory testing, software modeling and limit equilibrium.

2.2.1 Laboratory Testing

Several series of laboratory tests were described in the literature and are described below. Centrifuge model tests in particular were helpful in understanding how earth pressures affecting on retaining wall. Moreover, the centrifugal model was performed for retaining wall at rest condition to verify the arching theory by Janssen, 1895.

Janssen, 1895 was one of the first engineers to describe the behavior of granular material in a confined space. He was interested in the pressures exerted on a silo by granular materials such as grain or corn. He built a model silo and measured the weight of the corn at the bottom of the silo. The results showed that the weight at the bottom of the silo was

less than the weight of the corn in the silo. Janssen hypothesized that the weight of the corn was transmitted to the side walls. Because his experiments were performed with granular materials, his findings were also applicable to granular soils such as sand and gravel. Janssen's hypothesis that the weight of granular materials is transmitted to the side walls of a container became widely accepted and is often referred to as "Janssen's arching theory" or simply "arching theory" today (Spangler & Handy, 1982).

Horizontal earth pressures in soil resulting from arching effects are addressed by Spangler and Handy (1982). They suggest the horizontal earth pressure coefficient (k') is given by the following equation based in part on Janssen's original arching theory

$$k' = \frac{1}{2\tan(\delta)}\left(\frac{w}{z}\right)\left[1-\exp\left(-2k_o\frac{z}{w}\right)\tan(\delta)\right]$$

where w is the width of the constrained space, z is the depth of the point of interest below the top of the wall, δ is the interface friction angle between the soil and wall, k_o is the horizontal earth pressure coefficient which is defined k_o = 1-sin(ϕ), and γ is the unit weight of the backfill.

To verify the arching theory, Frydman and Keissar (1987) presented an early centrifuge model to study the earth pressures in a confined space. They examined the horizontal earth pressures transferred to a rigid retaining wall by granular fill confined between a wall and an existing stable face. They performed a series of centrifuge tests on model retaining walls with no reinforcement. A schematic of the model retaining wall is shown in Figure 2.5. Tests were performed for wall aspect ratios (w/H) ranging from 0.10 to 1.1, and horizontal earth pressures against the wall facing were measured. Tests were performed on a rigid wall that was prevented from moving during the experiment.

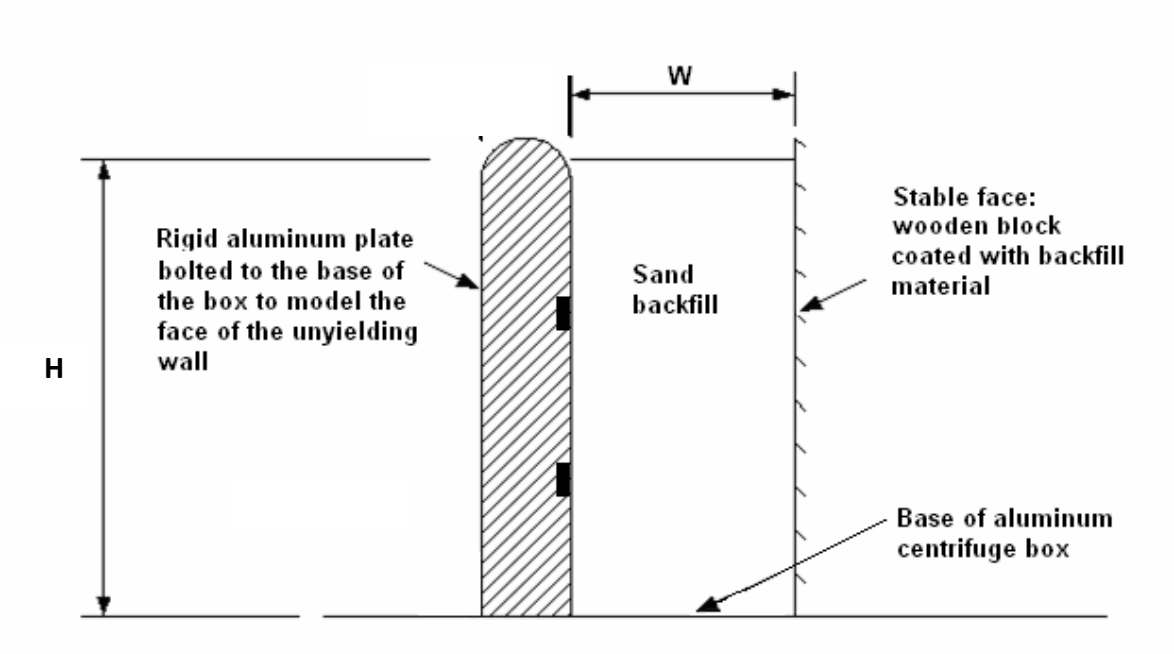

Figure 2.5: Schematic illustration of non-deformable wall used in centrifuge tests by Frydman and Keissar (1987)

The variation in horizontal earth pressure coefficients at two locations below the top surface of the wall measured from tests performed by Frydman and Keissar for wall aspect ratios equal to 1.10 and 0.10 is shown in Figure 2.6. They carried out the test at different soil densities. The results are presented as normalized values. The depth is expressed as a non-dimensional depth z/H where z is the depth below the top of wall and H is the height of the wall. Similarly, the horizontal earth pressures acting on the wall are represented by a non-dimensional horizontal earth pressure coefficient k. The values of k were calculated by dividing the measured horizontal stresses (σ_h) by the overburden pressure (γz). It was found that the earth pressure coefficients decreased with depth and as the wall aspect ratio decreased. The values of the horizontal earth pressure coefficients calculated by Spangler and Handy's equation are shown in Figure 2.7 which agrees well with the values measured by Frydman and Keissar (1987). (Frydman and Keissar, 1987).

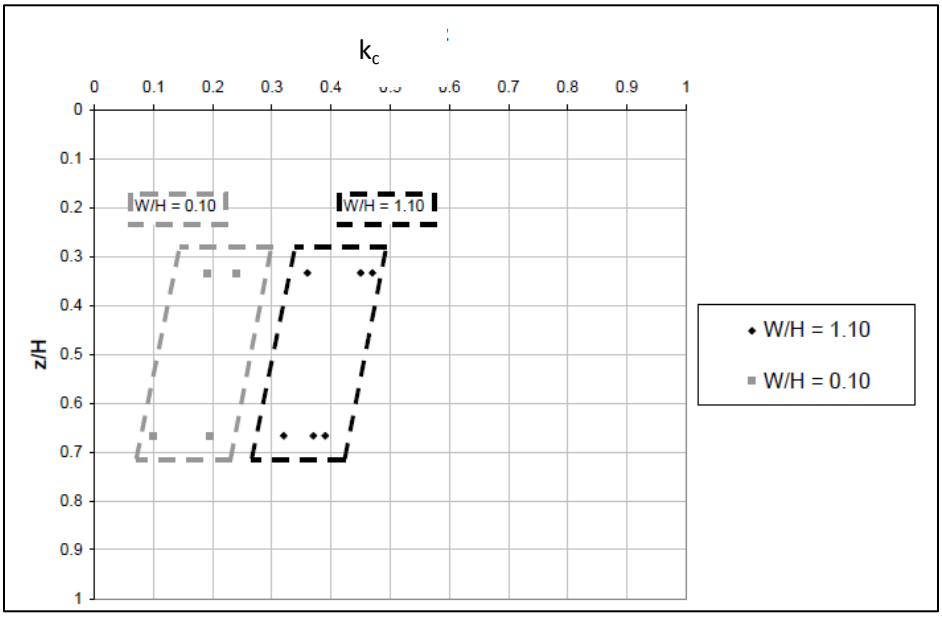

Figure 2.6: Variation in horizontal earth pressure coefficients (k_c) with the non-dimensional depth (z/H) performed by Frydman and Keissar

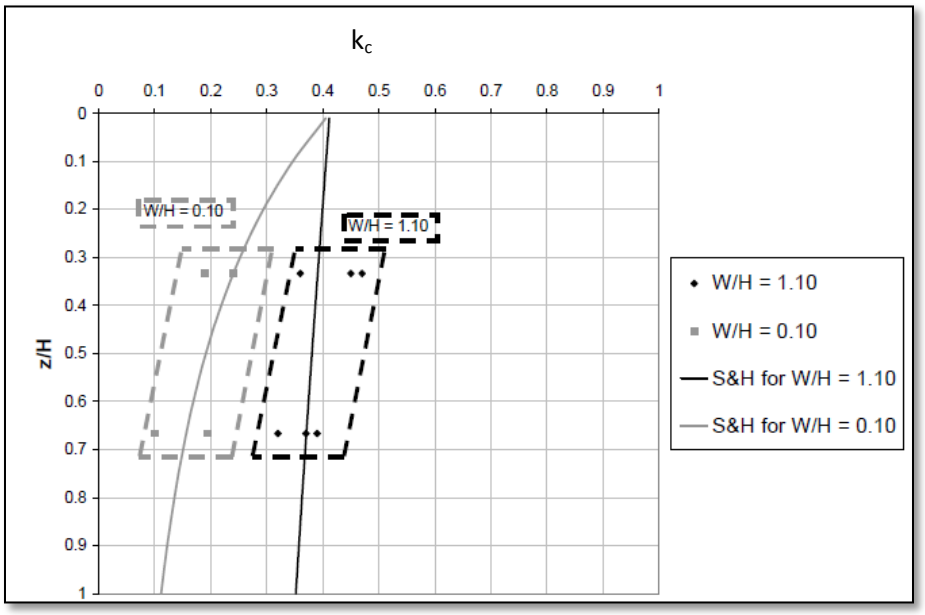

Figure 2.7: Horizontal earth pressure coefficients (k_c) with the non-dimensional depth (z/H) performed by Frydman and Keissar and values of k_c using Spangler and Handy's equation

Additionally, Take and Valsangkar, 2001 also studied the earth pressures in a confined space using centrifuge tests. A schematic of their centrifuge testing apparatus is shown in

Figure 2.8. They conducted an extensive series of experiments using pressure cells in centrifuge tests. The pressure cells were used to measure horizontal earth pressures behind non deformable retaining walls in a confined space. They investigated the influence of two primary variables: relative density of the backfill and the wall aspect ratio (w/H). Relative densities of the backfill equal to 34 and 79 percent were used in the experiments. The earth pressure cells were connected to the opposite wall, which was made of aluminum and represented the (non-deformable) retaining wall (Take and Valsangkar, 2001).

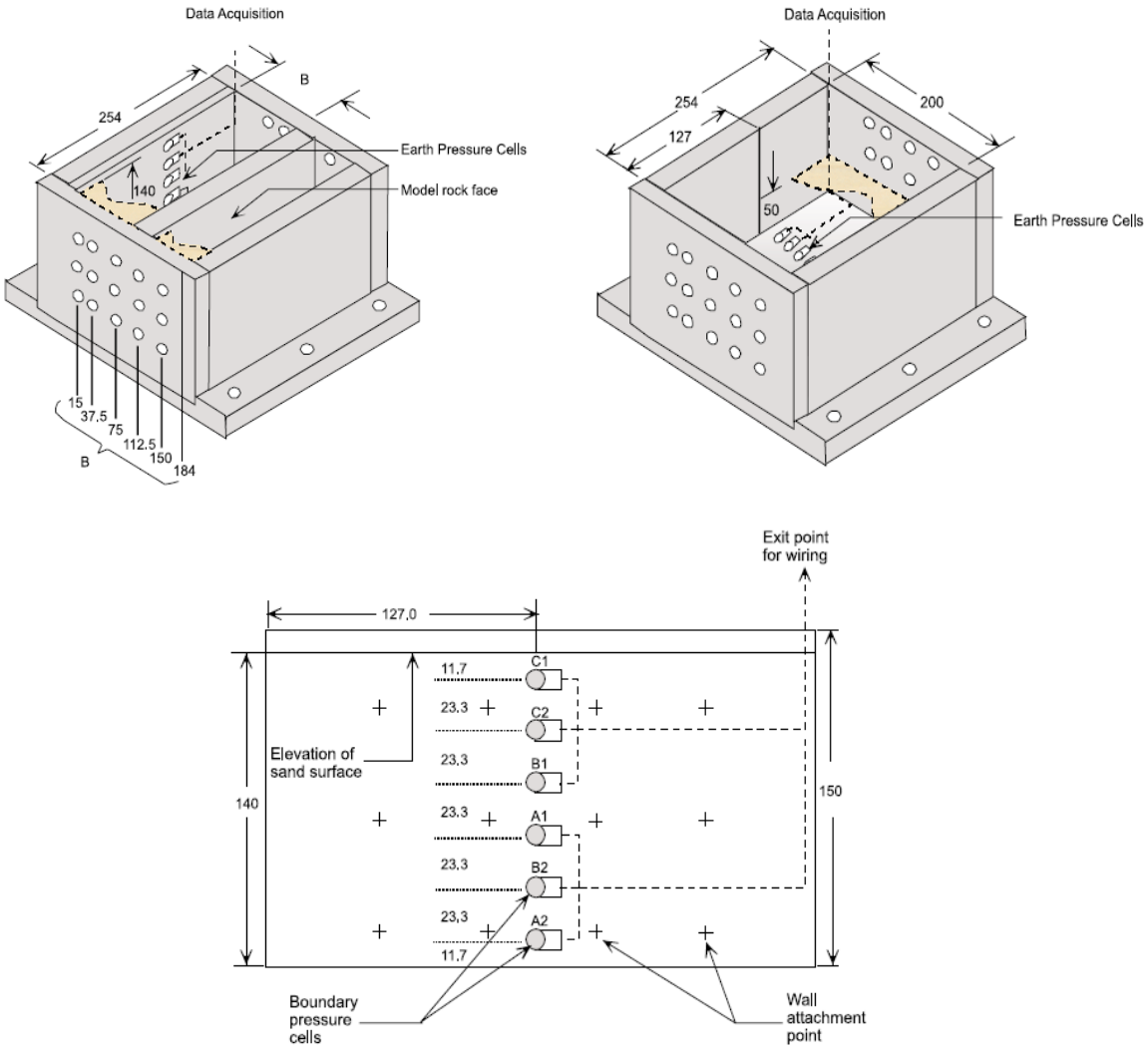

Figure 2.8: Schematic illustration of non-deformable wall used in centrifuge tests by Take and Valsangkar, 2001

Take and Valsangkar, 2001 tests showed that the horizontal earth pressures decreased as the relative density increased, apparently as a result of the angle of internal friction increasing from 30° to 36. Additionally, the results indicated that the horizontal earth pressures generally decreased as the wall aspect ratio decreased.

The variation in horizontal earth pressure coefficients (k) with non-dimensional depth (z/H) measured in Take and Valsangkar's centrifuge tests for wall aspect ratios (w/H) of 0.54 and 0.11 is shown in Figure 2.9. The depth is expressed as a non-dimensional depth z/H where z is the depth below the top of wall and H is the height of the wall. Similarly, the horizontal earth pressures along the wall are represented by a non-dimensional horizontal earth pressure coefficient k. The values of k were calculated by dividing the horizontal stress (σ_h) by the overburden pressure (γz). The earth pressure coefficients measured in the test with a wall aspect ratio equal to 0.11 are generally less than those measured in the test with a wall aspect ratio equal to 0.54. Also, the values of k decreased with depth below the top of the wall. Take and Valsangkar also concluded that the measured horizontal earth pressures acting on the non-deformable model walls showed good agreement with values computed using Spangler and Handy's equation (Take and Valsangkar, 2001).

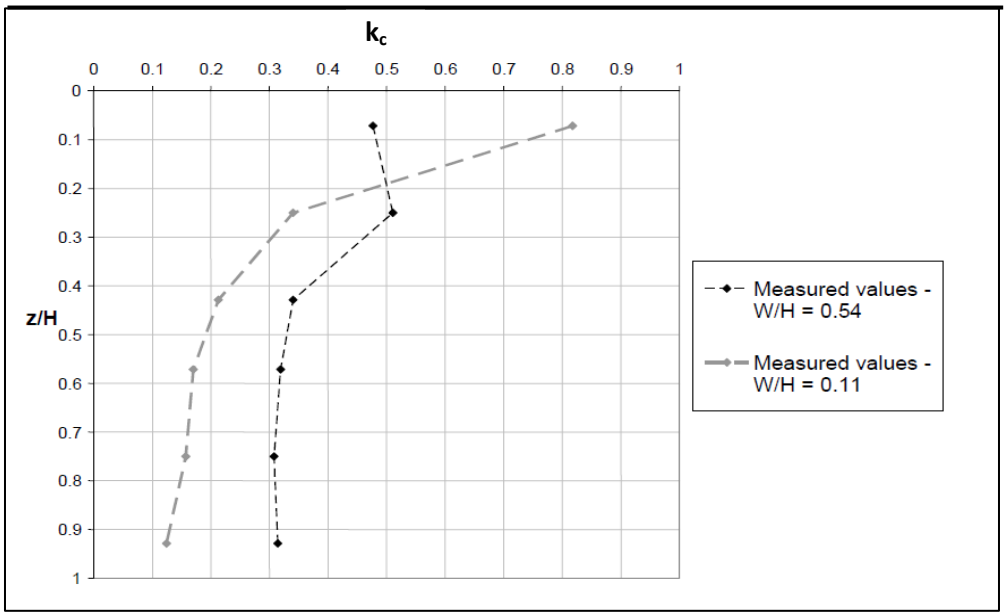

Figure 2.9: Horizontal earth pressure coefficients (k_c) with the non-dimensional depth (z/H) with wall aspect ratios (w/H) (Take and Valsangkar, 2001)

2.2.2 Limit Equilibrium Analysis

Leshchinsky & Hu, 2003 and Lawson and et al, 2005 performed limit equilibrium analysis to study the effect of backfill width ratio on the horizontal earth pressure coefficient. Results of both studies are presented below.

Leshchinsky & Hu, 2003 performed a series of limit equilibrium analyses of walls placed in a confined space. They considered the geometry shown in Figure 2.10. They varied the wall aspect ratio at the bottom of the wall (b/H) and the inclination of the back slope (m) (Leshchinsky and Hu, 2003).

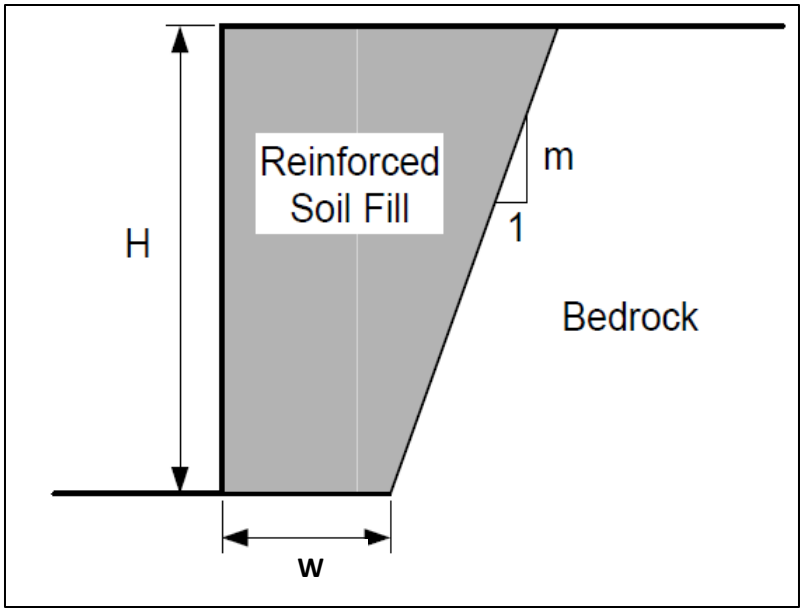

Figure 2.10: Wall configuration considered by Leshchinsky & Hu, 2003

The purpose of the limit equilibrium analyses was to calculate the force required for equilibrium with the shear strength of the soil fully developed. Thus, the required force corresponds to the conditions normally assumed for Rankine active earth pressures. They assumed circular slip surfaces. The resultant earth pressure force was assumed to act at the lower third point of the wall.

Based on their limit equilibrium analysis, Leshchinsky & Hu, 2003 presented a series of design charts shown in Figures 2.11 through 2.13 for the earth pressure coefficient expressed as a ratio of the calculated horizontal earth pressure coefficient, k_c, to the Rankine active earth pressure coefficient, k_r defined in the Equation.

$$k_r = \tan^2\left(45 - \frac{\phi}{2}\right)$$

The calculated earth pressure coefficient was determined by applying the following equation,

$$k_c = \frac{P_a}{\frac{1}{2}\gamma H^2}$$

Where P_a is the value of the resultant force found from limit equilibrium analyses, γ is the total unit weight of the fill, and H is the height of the wall. The ratio of the calculated horizontal earth pressure coefficient (k_c) to the Rankine active earth pressure coefficient (k_r) was designated as R ($R = k_c/k_r$).

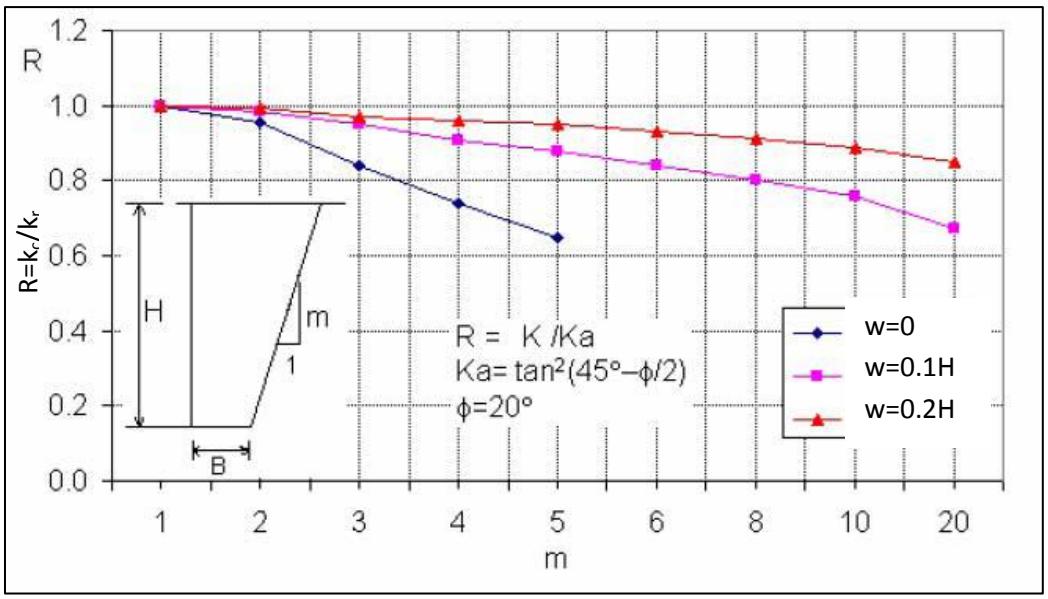

Figure 2.11: Design charts developed for an angle of internal friction equal to 20° **(**Leshchinsky & Hu,2003**)**

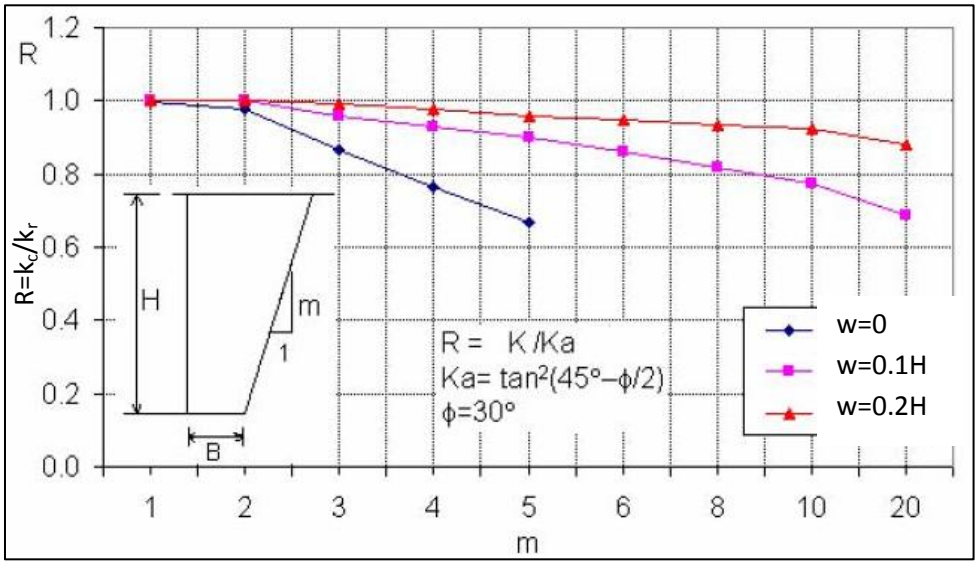

Figure 2.12: Design charts developed for an angle of internal friction equal to 30° (Leshchinsky & Hu,2003)

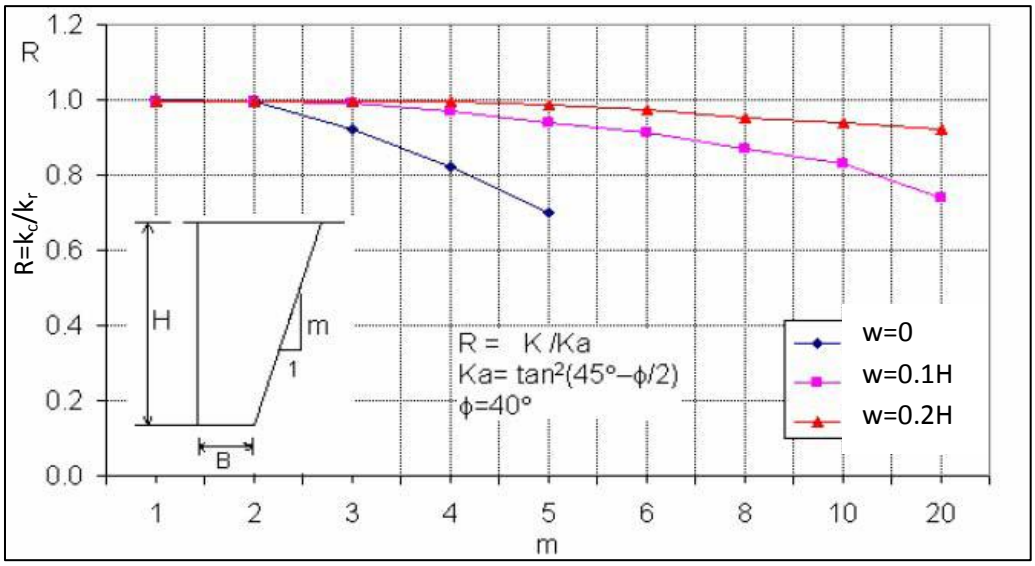

Figure 2.13: Design charts developed for an angle of internal friction equal to 40° (Leshchinsky & Hu,2003)

Leshchinsky & Hu, 2003 showed that as the backfill width ratio (w/H) decreased, the value of R also decreased. They also showed that as the inclination of the back slope increased, i.e., the back slope became more vertical, the value of R decreased.

Additionally, Lawson & Yee, 2005 developed charts for earth pressure coefficients using limit equilibrium procedures. They used the same geometry as Leshchinsky & Hu, 2003

as shown in Figure 2.10. They considered both planar and bilinear slip surfaces, as shown in Figure 2.14. Lawson & Yee, 2005 showed that the horizontal earth pressures were less than or equal to the Rankine active earth pressures when the wall aspect ratio was less than or equal to 70 percent of the wall height, i.e., w/H < 0.70. They also showed that the horizontal earth pressure coefficient decreased as the wall aspect ratio decreased as shown in Figure 2.15 (Lawson & Yee, 2005).

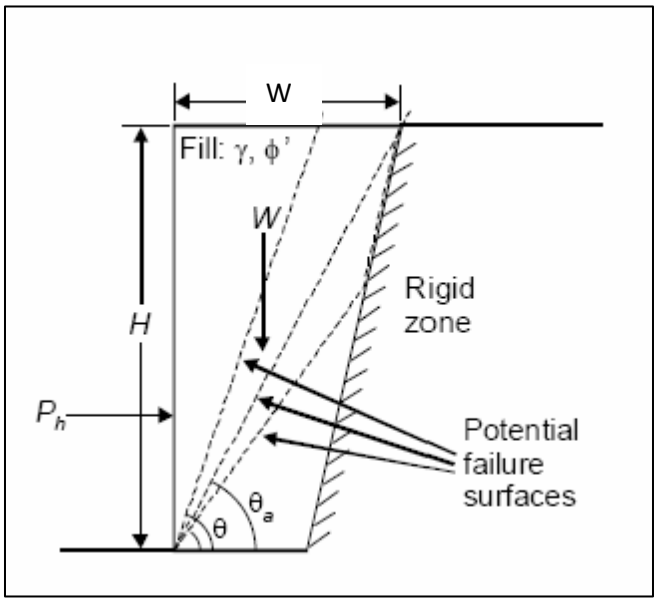

Figure 2.14: Forces acting on wall face and potential failure surfaces analyzed by (Lawson & Yee,2005)

The variation of the horizontal earth pressure coefficient as a function of the wall aspect ratio (w/H) and angle of different values of internal friction is shown in Figure 2.15. Lawson et al, 2005 showed that both the friction angle of the backfill and the wall aspect ratio govern the magnitude of the horizontal earth pressure coefficient acting on the face of the wall.

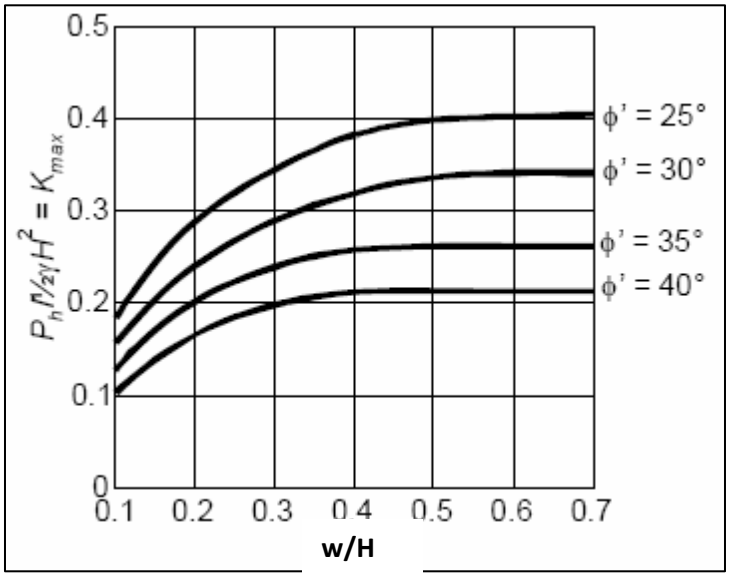

Figure 2.15: Maximum horizontal force coefficients for ϕ = 25°, 30°, 35° and 40° (Lawson & Yee, 2005**)**

2.2.3 Finite Element Analysis

Yang & Liu, 2007 performed a finite element analysis to investigate the earth pressures behind walls with less than the normal width. The earth pressures at different stages (at rest or active condition) and different locations (along the wall face or along the center of the wall) were studied.

The finite element program (Plaxis) was used to conduct the numerical analysis in Yang & Liu, 2007 study. Figure 2.16 shows the finite element model simulating at-rest condition. Figure 2.17 shows the finite element model for active condition. In Figure 2.16, a horizontal fixity was employed on facial structure to prevent it from horizontal movement. The horizontal fixity guarantees the wall keeping in at-rest condition. In Figure 2.17, a prescribed displacement is added to rotate the wall facing structure outward and force the backfill in the wall to reach failure stage to simulate active condition (Yang & Liu, 2007).

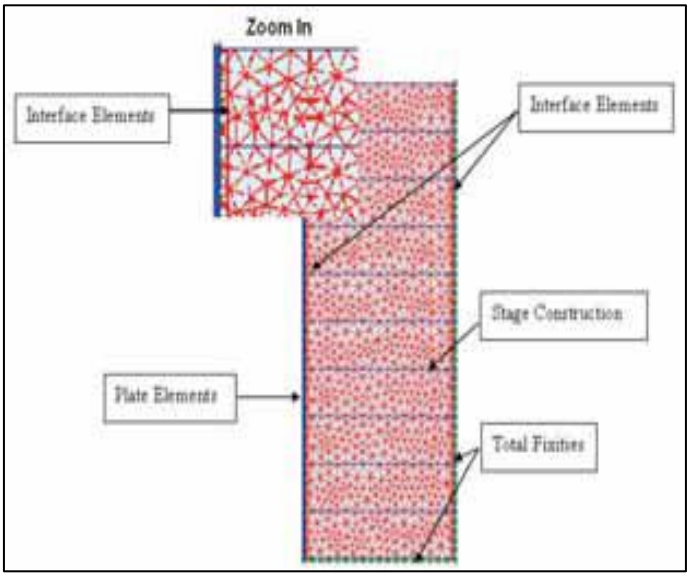

Figure 2.16: Finite element meshes for at-rest case (Yang & Liu, 2007)

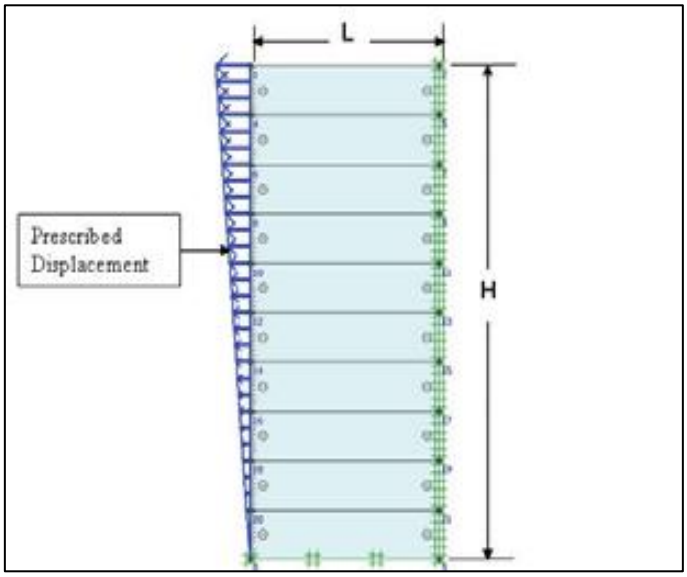

Figure 2.17: Finite element meshes for at-active case (Yang & Liu, 2007)

The finite element meshes are composed of 15-node triangular elements to model the soil. This 15-node triangle is considered a very accurate element that has produced high quality stress results for difficult problems. The mesh was set as "Fine", which would generate around 500 triangular elements for a given geometry. Mohr-Coulomb model was chosen as the soil constitutive model. Total fixities were used to represent the stable face. Plate elements were used to represent the facial structure of retaining wall.

The results of finite element analysis indicated that the trend of the decrease of earth pressures as the decrease of wall aspect ratios was observed through this study. This decreasing tendency could be ascribed to arching effects and boundary constraint. Arching effect was more major in at-rest condition than in active condition in which boundary constraint dominated. Both of Figures 2.18 and 2.19 show the results.

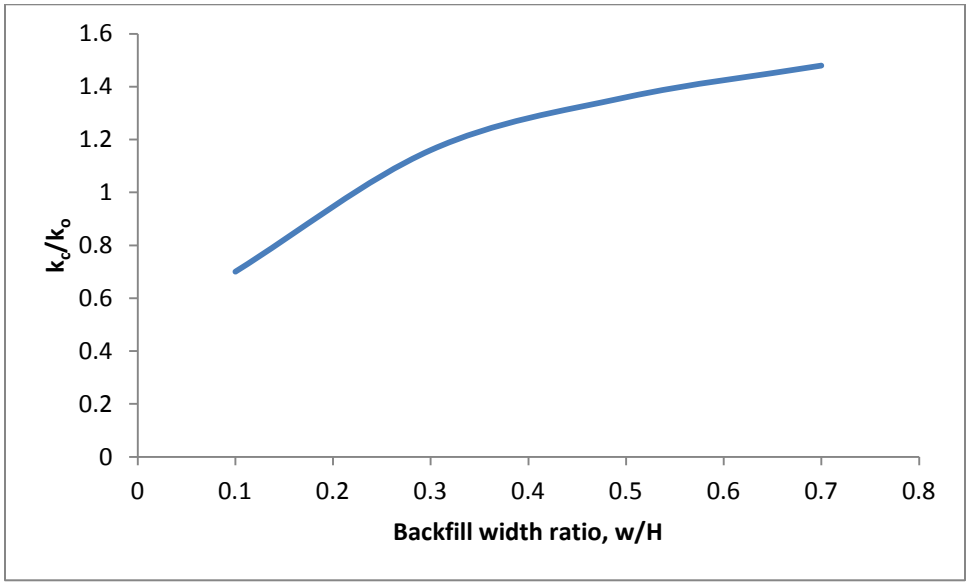

Figure 2.18: Normalized equivalent earth pressure coefficients for at-rest case (Yang & Liu, 2007)

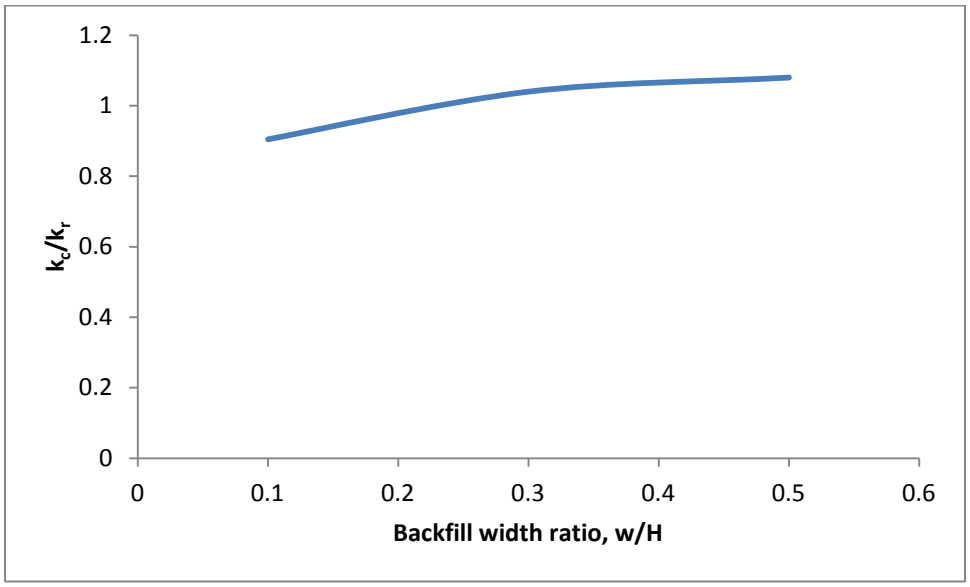

Figure 2.19: Normalized equivalent earth pressure coefficients for at-active case (Yang & Liu, 2007)

Fan et al, 2010 investigated active earth pressures on rigid retaining walls built near rock faces. The fill space behind the wall was limited due to the presence of the rock face. The finite element method was used to carry out the analysis. Rock faces behind the fill space with various sloping conditions and with various distances from the wall were taken into account in the FE analysis (Fan et al, 2010).

The non-linear finite element program (plaxis) was used to analyze the earth pressure at-rest and active conditions. Soil elements used in this study were six-node triangular elements. The Mohr–Coulomb constitutive model was used to model the stress–strain behavior of soils. Figure 2.20 shows plaxis model.

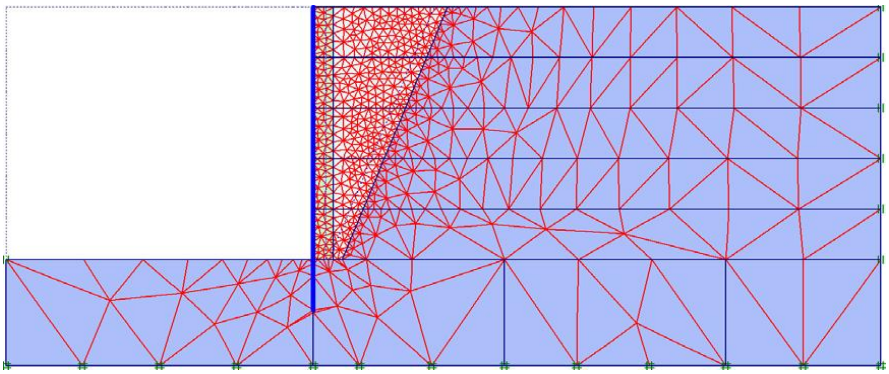

Figure 2.20: The finite element mesh for a retaining wall with limited backfill space. (Fan et al, 2010)

The coefficients k_c of the active earth pressures on rigid walls near rock faces were considerably less than the Coulomb solution and decreased with increasing inclination of the rock face. A simple relationship between the normalized coefficient ($k_c/k_{a(Coulomb)}$) of active earth pressures on walls near rock faces and the rock inclination was obtained at different backfill width. The $k_c/k_{a(Coulomb)}$ value decreased with the decreasing backfill width ratio of the fill space.

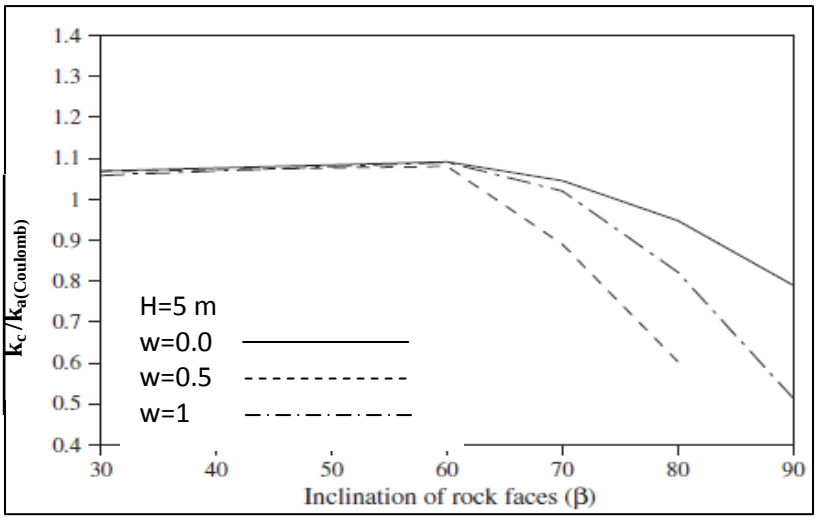

Figure 2.21: Variation of the coefficient of active earth pressures ($k_c/k_{a(Coulomb)}$) with the inclination of rock faces at various fill widths (w)

Chapter 3
Research Methodology

This chapter presents the research methodology that was followed in this thesis. The study involved two major works, which are numerical modeling using plaxis software and the experimental work. The research started by reviewing all previous literature related to this research. Then, these studies have been summarized in a brief way with its results. The methodology followed in this research is summarized in Figure 3.1.

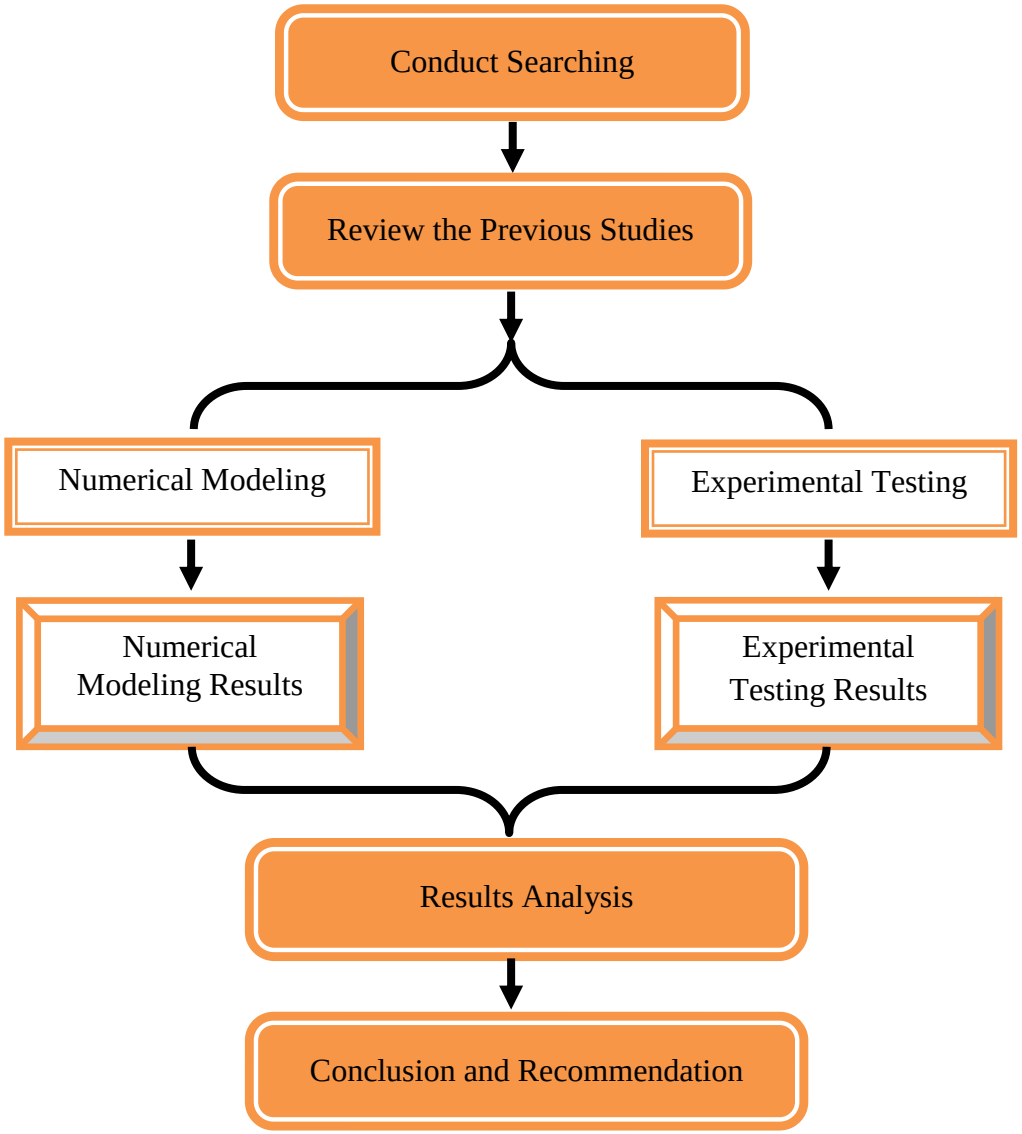

Figure 3.1: Methodology of the research

3.1 Numerical Modeling

PLAXIS software is a program that applies the principles of the finite element method (FEM) to soil models. It is widely used in practice because of its simplicity, user-friendliness and reliability. The program is available in several packages and the one used in this thesis is the PLAXIS 2D, which is designed to solve two dimensional plane-strain problems. It was first developed at the technical university of Delft in the Netherlands as a project to evaluate possible movements of the Oosterschelde-dam.

This software program is designed to be used primarily by practicing engineers, providing a user-friendly and interactive interface through four programs: Input, Calculation, Output, and Curves. The following section gives a brief summary about the Plaxis features used for modeling (Brinkgreve, 2002)

3.1.1 Geometry

The generation of finite element model begins with the creation of a geometry model, which is a representation of the problem of interest. A geometry model consists of points, lines and clusters. Points and lines are entered by the user, while clusters are generated by the program. It is recommended to start the creation of a geometry model by drawing the full geometry contour. In addition, the user may specify material layers, structural objects, lines used for construction phases, loads and boundary condition. Figure 3.2 illustrates the geometry model to the case study.

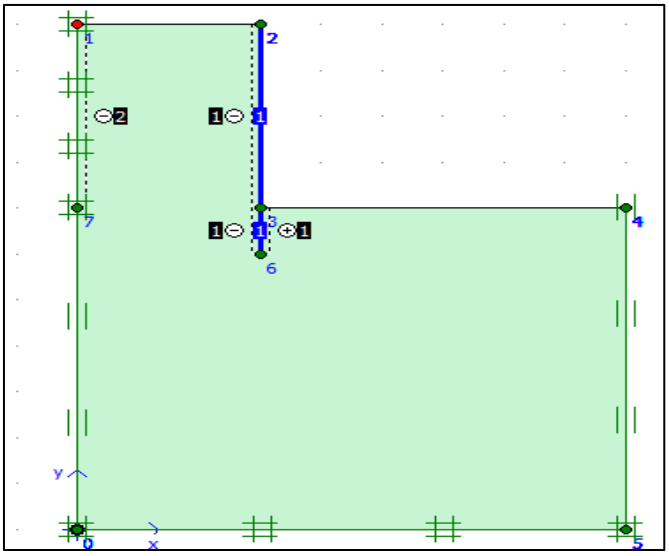

Figure 3.2: Geometry Model

3.1.2 Boundary condition

Boundary condition can be found in the center part of the second toolbar and in the Load menu. This menu contains the options to introduce distributed loads, lines loads or point loads, prescribed displacement and fixities, total fixities, horizontal fixities or vertical fixities. These options can be applied at the model boundaries as well as inside the model. It is noteworthy that the fixities are prescribed displacement equal to zero. These conditions can be applied to geometry line as well as geometry point.

Regarding this research, a total fixity was defined at the base of the model and the rock face. Additionally, the horizontal fixities were developed at both right and left boundaries. The interface element is also defined to have the value of 0.67, since the friction angle between retaining wall and soil material is two third (2/3) the soil friction angle (Das, 2011)

3.1.3 Mesh generation

When the geometry model is complete, the finite element model or (mesh) can be generated. The basic type of element in a mesh is the 15- node triangular element or 6-node triangular element. In addition, to these elements, there are special elements for structural behavior (plates, geogrids and anchors). The mesh generation takes full account of the position of points and lines in the geometry model, so that the exact position of layers, loads, and structures is accounted for in the finite element mesh. The required input for the mesh generator is a geometry model composed of points, lines and clusters, of which the clusters (area enclosed by lines) are automatically generated during the creation of the geometry model. Geometry lines and points may also be used to influence the position and distribution of elements. Figure 3.3 illustrates the result of meshing.

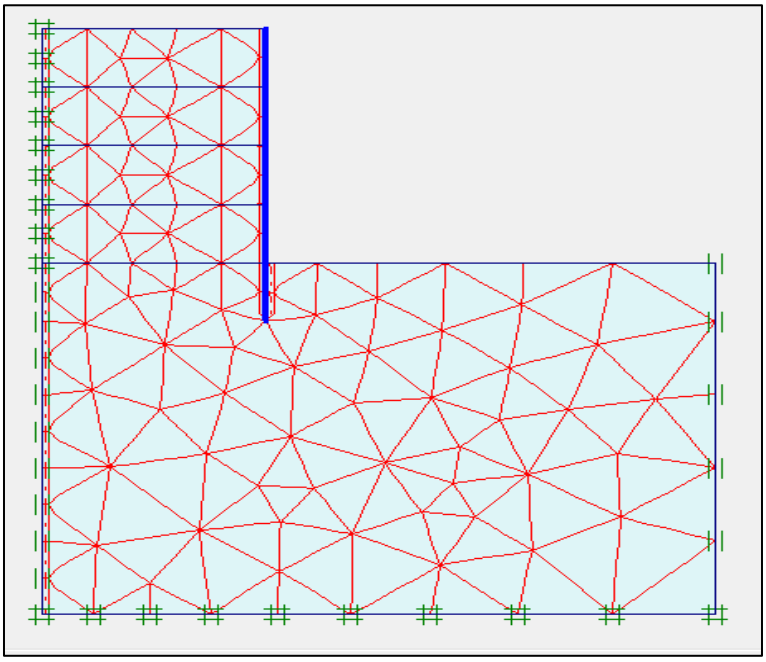

Figure 3.3: Result of Meshing

3.1.4 Initial condition

Once the geometry model has been created and the finite element mesh has been generated, the initial stress state must be specified. This is done in the initial conditions part of the input program. The initial conditions consist only mode for the specification of the initial geometry configuration and the generation of the initial effective stress. The mode for the generation of initial water pressures (water conditions mode) was neglected since the water influence out of our research.

3.1.5 Calculations

After the generation of a finite element model, the actual finite element calculations can be executed. Therefore, it is necessary to define which types of calculations are to be performed and which types of loadings or construction stages are to be activated during the calculations.

3.1.6 Output results

Once the calculation has been completed, the results can be evaluated in the Output program. In the Output window, can view stresses in the full geometry as well as in cross sections.

3.2 Experimental testing

To verify the obtained results from numerical modeling using plaxis software program, experimental work was carried out using centrifugal modeling. In addition a Geo-kon device was used to measure the soil pressure adjacent behind retaining wall. The following sections describe the centrifugal model with more details and the experimental work description.

3.2.1 Backfill material

Sandy soil was used as a backfill material for centrifugal model. The backfill behind the retaining wall was filled regularly at a specified distance up to 10 cm to ensure the homogeneity of backfill. Moreover, some tests were conducted to define the backfill properties namely, unit weight and direct shear. The results of these tests are mentioned in chapter four regarding results presentation and analysis.

3.2.2 Preparation of centrifugal model

The model was built after reviewing the previous literature. It was made of wooden material with 2.5 cm thickness as shown in figure 3.4. This type of material was used to ensure the rigidity of the retaining wall as rock face. Additionally, the wooden material is considered simple for work implementation.

Moreover, the determination of centrifugal model size was governed by the pressure cell size so that, the model was designed to be consistent with available cell diameter. The pressure cells were used in the present study have a diameter of 22 cm and the model was sized to be more than four times the cell pressure diameter to avoid the interference. Accordingly, the model was constructed to have a dimension of 1.2m height and 1m width. The third dimension which represents the backfill width was varied with maximum value reaches to 1.44 m.

The centrifugal model has a box-shaped. One side of this box instrumented the retaining wall. The opposite side of the retaining wall representing the rock face. The retaining wall model was pinned at the base to prevent the sliding and match the wall displacement for actual case, since the movement at the base is zero and free at the top. In addition to that, the rock face model was fixed at a certain backfill width ratio. The backfill width is varied between 0.24 m to 1.44 m with increment of 0.24m.

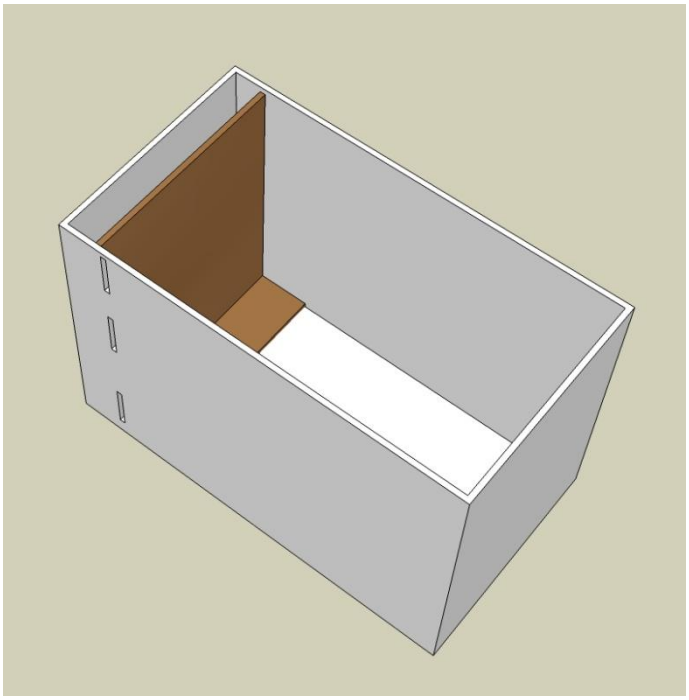

Figure 3.4: Physical Model

3.2.3 Instruments used in the experiments

The devices used in the experiments of our study are manufactured in Geokon Company for Geotechnical Instrumentation in USA. Two vibrating wire devices were used in the experiments. The first one device was used for measuring vertical and horizontal earth pressure while the second one is the readout box. Details on these devices are described in following sections.

1.Vibrating Wire Earth Pressure Cell

Pressure cell device was used to measure earth pressures behind the retaining wall. Horizontal and vertical earth pressures were measured using this device.

a. Applications

Earth Pressure Cell provide a direct means of measuring total pressures, i.e. the combination of effective soil stress and pore water pressure, in the following cases:

- Bridge abutments;
- Diaphragm walls;
- Fills and embankments;

- Retaining walls surfaces and;
- Sheet piling and;

This device also used to measure earth bearing pressures on footings. Figure 3.5 shows earth pressure cell, which is used in measurement of horizontal and vertical earth pressures in our case study.

Figure 3.5:Earth Pressure Cell

b. Operating Principle

Earth Pressure Cell are constructed from two stainless steel plates welded together around their periphery and separated by a narrow gap filled with hydraulic fluid. External pressures squeeze the two plates together creating an equal pressure in the internal fluid. A length of stainless steel tubing connects the fluid filled cavity to a pressure transducer that converts the fluid pressure into an electrical signal transmitted by cable to the readout Location.

c. Technical Specifications

Table (3.1) shows the technical specifications of earth pressure cell used in our case study.

Table 3.1: Technical Specifications of Vibrating Wire Earth Pressure Cell

Earth Pressure Cell	
Transducer	Vibrating Wire
Standards Cell Dimensions (D)	220 mm
Transducer Dimension (LxD)	150x25 mm
Material	304 stainless Steel

d. Theory of Operation

Earth Pressure Cells, sometimes called Total Pressure Cells or Total Stress Cells are designed to measure stresses in soil or the pressure of soil on structures. Cells will respond not only to soil pressures but also to ground water pressures or to pore water pressure, hence the term total pressure or total stress. A simultaneous measurement of pore water pressure (μ), using a piezometer, is necessary to separate the effective stress (σ') from the total stress (σ) as defined by Terzaghi's principle of effective stresses where;

$$\sigma = \sigma' + \mu$$

Earth pressure cell which is described here is a hydraulic type; two flat plates are welded together at their periphery and are separated by a small gap filled with a hydraulic fluid. The earth pressure acts to squeeze the two plates together thus building up a pressure inside the fluid.

2. Initial Readings

Initial readings must be taken and carefully recorded. Take the initial readings while the cell is in position, just prior to it being covered by fill.

3. Pressure Calculation

The basic units utilized by Geokon for measurement of data from Vibrating Wire Earth Pressure Cells are "digits". To convert digits to pressure the following Equation applies;

$$P = (R_o - R_1) \times C$$

The Initial Reading (Ro) is normally obtained during installation (usually the zero reading) and (C) is the calibration factor.

3.2.4 Experimental work description

A series of experimental work were performed to measure the soil pressure behind retaining wall. Accordingly, three locations were allocated to measure the soil pressure. The backfill width ratio (w/H) was varied between 0.2 to 1.2 with increment of 0.2. For each backfill width ratio, the soil pressure was measured at three different locations.

3.3 Results analysis and discussion

According to the output results from plaxis model, a suitable relation between these results has been conducted and studied the main factors that have a direct effect on lateral earth pressure coefficient. The main factors has been considered during this research are the effect of width of backfill related to retaining wall height, besides the influence of varied friction angles with a certain backfill width ratio. These results have been compared with other obtained results that were taken from experimental work.

All of these results are presented by charts and compared with other previous related studies in chapter four

Chapter 4
Results and Analysis

Effect of soil pressure behind retaining wall is considered a high interested and very important for retaining wall design consideration. In this research, the emphasis was on retaining wall in case of narrow backfill at active condition. Accordingly, a number of tests were performed at different ratios of backfill width to height (w/H). Two different categories have been considered throughout this research, which are;

- **Theoretical Study:**

  Theoretical study has been conducted using a numerical modeling (plaxis software program). The main purpose of this study was to investigate the lateral earth pressure effect on retaining wall in case of narrow backfill, so that a different cases have defined by plaxis program.

  Plaxis is a finite element program for geotechnical applications in which soil models are used to simulate the soil behavior. Many of geotechnical problems could be analyzed by plaxis program i.e. retaining walls, sheet piles, earth dams, tunnels and others. Although many of tests and validation have been performed, it cannot be guaranteed that the plaxis code is free of errors. Moreover, the development of plaxis began in 1987 at Delft University of Technology as an initiative of Dutch Ministry of Public Works and Water Management. The initial purpose was to develop an easy-to-use 2D finite element code for the analysis of river embankments on soft soils of Iowlands of Holland.

  Further details about plaxis modeling are mentioned in chapter 3 which describes the research methodology for this study.

- **Experimental Work:**

  The main purpose of the experimental work was to verify and validate the results that have been obtained from numerical modeling. Experimental work has been performed using a centrifugal model. This model was made of wooden material with box-shaped. Furthermore, Geo-kon device was

employed to measure the vertical and horizontal soil pressure. The measurements were conducted at three different locations behind the retaining wall for each backfill width.

Moreover, the sandy soil was used as a backfill material behind the retaining wall. Some tests have been conducted to define the soil properties.

Results and discussion of both theoretical study and experimental work will be presented in this chapter. Also, a comparison between these results is presented. Figure 4.1 shows the sequence of data results presentation.

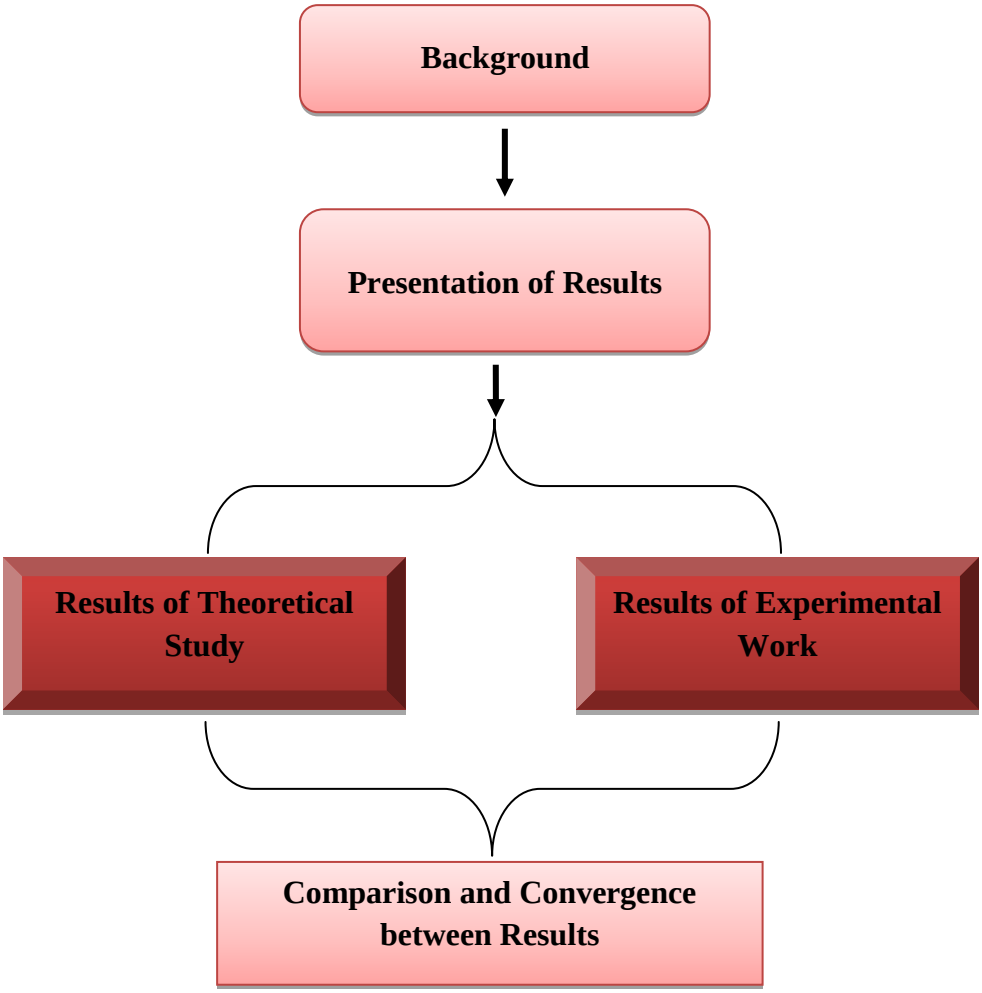

Figure 4.1: Sequence of data results presentation

4.1 Theoretical Study

Plaxis software program was utilized to conduct the numerical modeling in this study. A typical geometry of the backfill zone used in this research is shown in Figure 4.2.

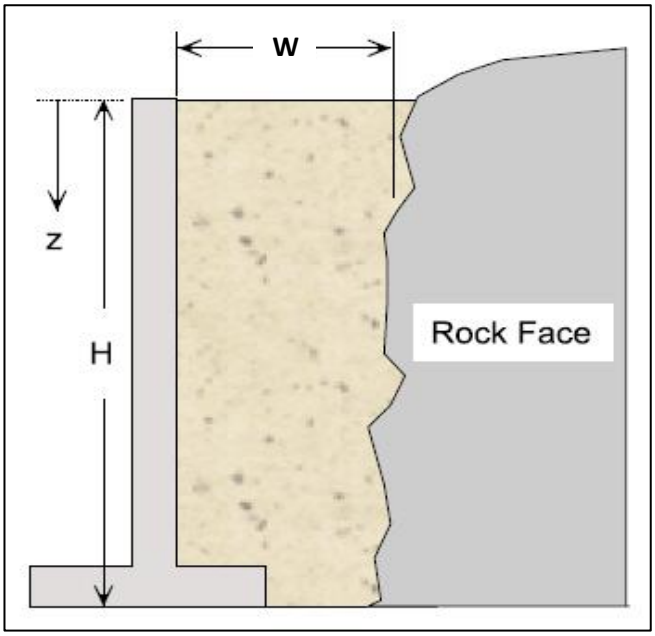

Figure 4.2: Typical geometry of case study (Yang & Liu, 2007)

The wall used in the analysis represents a rigid reinforced concrete wall, (i.e., no bending during wall movement), in the FE model. To investigate the influence of the backfill-space geometry on the behavior of active earth pressures, the distance (w) between the wall and the rock face were varied in the numerical analysis.

4.1.1 Modeling of backfill, walls, and interfaces

Sandy soil model was used as a backfill material behind retaining wall. Soil elements used in this study were modeled to have 15-node triangular elements. This 15-node triangle is considered a very accurate element that has produced high quality stress results for difficult problems. The Mohr–Coulomb constitutive model was used to model the stress–strain behavior of soils. This model requires five parameters, i.e., Young's modulus (E), Poisson's ratio (ϑ), friction angle (ϕ), cohesion (c), and dilatancy angle (φ). The dilatancy angle (φ) is normally used in cohesionless materials and is dependent on the friction angle of the soil. For a soil material with friction angle greater than 30^0, the

soil tends to dilate at small strain conditions, where active earth pressures develop. The dilatancy angle (φ) is approximately equal to ϕ -30 (*where* ϕ *is the soil friction angle*), and it is used in the current study.

Interface elements between the wall and the backfill and between the rock face and the backfill were taken into account in the analysis. The interface element had a zero thickness in the finite element formulation. The material properties of the interface element were the same as those of surrounding soil elements, except that a strength reduction factor (R_{inter}), defined as the ratio of the interface strength to the shear strength of surrounding soils, was used for the interface element. The value of 0.67 was used for interface ratio between the retaining wall and the soil elements.

The rock formation behind the retaining wall was considered a stable face. Total fixity was used to simulate the rock face.

4.1.2 Results of Numerical Modeling

Two main factors were taken into consideration during the numerical modeling analysis, namely, the backfill width and the soil friction angle. Different backfill width ratios (w/H) ranging between 0.2 to 1.4 with increment of 0.2 were modeled to calculate the soil pressure against retaining wall. For each backfill width ratio, the soil friction angle has different magnitudes values ranging between 31^0-36^0. The next two sections will present the outcomes and results of theoretical study based on numerical analysis using plaxis software program.

1. ***Distribution of earth pressures behind retaining wall***

Based on numerical modeling using plaxis software program, it is clearly shown that the normalized earth pressure behind retaining was increased gradually with depth as shown in Figure 4.3. The pressure distribution has a triangular-shape where the pressure magnitude has zero value at the top of the wall and the maximum value at the base. This result indicates a good agreement with Rankine theory since the pressure distribution along the wall is defined by the following relation:$\sigma_h = k_a \gamma z$, where; $\boldsymbol{\sigma_h}$: *The horizontal earth pressure,* $\boldsymbol{k_a}$: *earth pressure coefficient for active condition,* $\boldsymbol{z}$: *interested depth*

Figure 4.3: Earth pressure distribution based on numerical modeling

2. Effect of fill-space geometry on active earth pressure

The location of the rock face behind retaining walls plays an important role in the mobilization of earth pressure on the wall. In this study, a different backfill width ratios ranging between 0.2 and 1.4 with increment of 0.2 were taken into consideration. Also, the soil friction angle ranging between 31^0 and 36^0 was considered.

In the following sections, a number of charts are provided showing the relation between the backfill width ratios and the lateral earth pressure coefficient ratio at different values of soil friction angle. The width is presented as non-dimensional quantity (w/H) where, (w) is the width of backfill and (H) is the wall height. Similarly, the lateral earth pressure coefficient along the wall face is represented by a non-dimensional lateral earth pressure coefficient (k_c/k_r), where (k_c) is the calculated coefficient by plaxis model and (k_r) is related to Rankine coefficient which could be obtained by the following equation:

$$k_r = tan^2\left(45 - \frac{\emptyset}{2}\right)$$

a. Earth Pressure Coefficient for Soil of $\phi=31^0$.

Figure 4.4 shows the relation between the equivalent lateral earth pressure coefficient as ratio of Rankine earth pressure coefficient and backfill width ratio for soil friction angle $=31^0$. The results clearly show that the equivalent lateral earth pressure coefficients are less than Rankine's coefficient by 18% to 6% when the backfill width ratio changed from 0.1 to 1.4. This difference is most likely due to the restricted space of backfill. Meanwhile the variation between (k_c/k_r) ratios considerably become small as the backfill width ratio is increased. Also, the earth pressure coefficient has an increasing tendency up (k_c/k_r) to 0.65, and then the tendency obviously becomes almost constant. A polynomial regression is defined to express the relation between (k_c/k_r) and (w/H) which has a correlation factor of 97%.

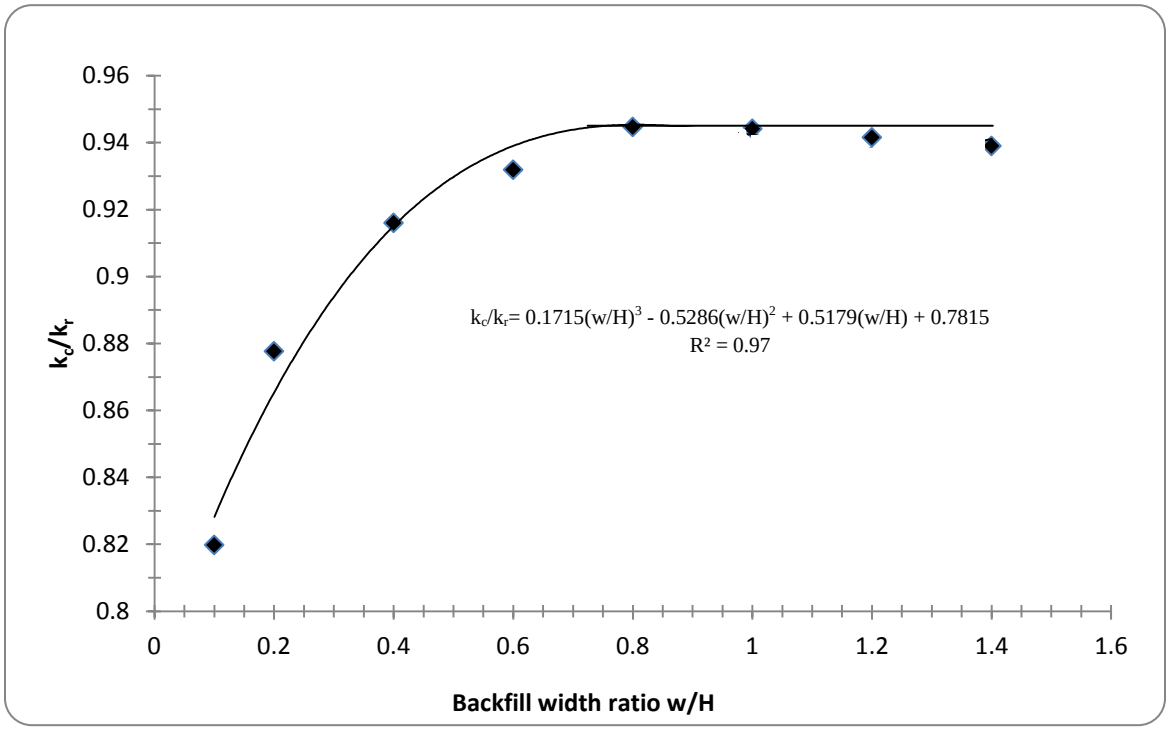

Figure 4.4: Relation between the backfill width ratio and k_c/k_r ratio (soil friction angle $=31^o$)

b. Earth Pressure Coefficient for Soil of $\phi=32^0$

A relationship between ratios of (k_c/k_r) and backfill width ratios for soil friction angle = 32^0 is presented in Figure 4.5. The figure shows that the lateral earth pressure coefficient

is increased as increasing the backfill width ratio up to (k_c/k_r) ratio of 0.6 then; the tendency becomes almost constant. The maximum magnitude value for (k_c/k_r) ratio is 0.94 which is obviously less than that computed using the Rankine theory.

Furthermore, Figure 4.5 shows that a polynomial regression matches the results were obtained by plaxis model with correlation factor of 98%. Indeed, a polynomial regression is a strong regression to express the relation between the equivalent earth pressure ratio and the backfill with ratio.

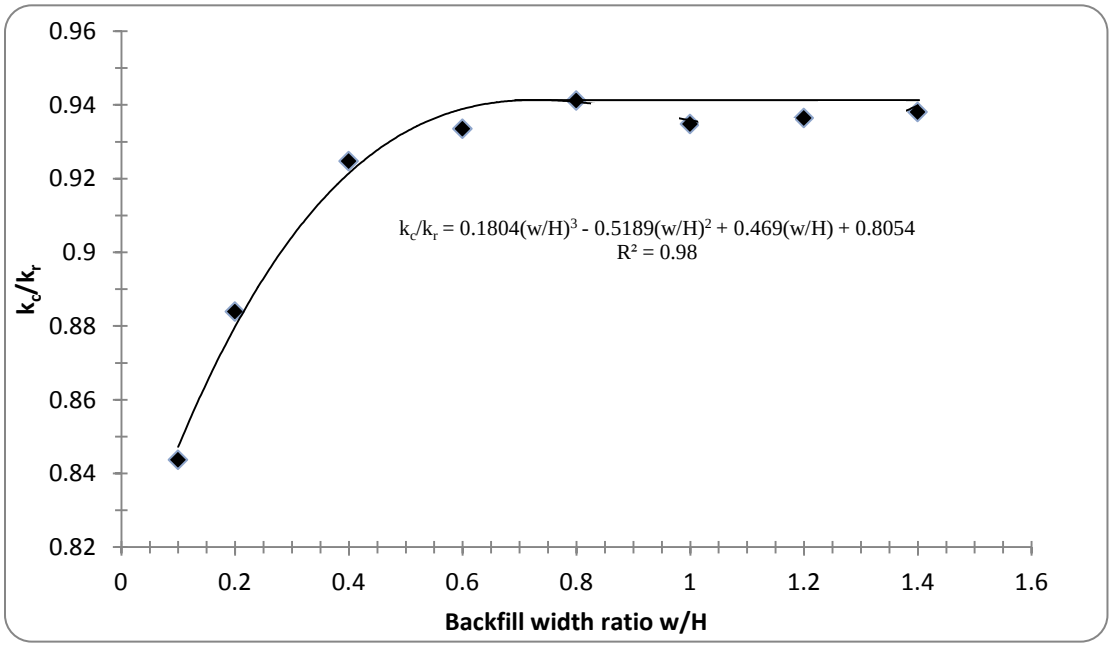

Figure 4.5: Relation between the backfill width ratio and k_c/k_r ratio (in case of soil friction angle =32^0)

c. Earth Pressure Coefficient for Soil of $\phi = 33^0$

Figure 4.6 shows the relation between the backfill width ratio and lateral earth pressure coefficient ratio for soil friction angle (ϕ) = 33^0, the results clearly show that the normalized equivalent lateral earth pressure coefficients are less than Rankine coefficient by 17% to 7% when the (w/H) ratio is changed from 0.1 to 1.4. Moreover, the variation of (k_c/k_r) ratios is decreased as the corresponding backfill width aspect ratio increased up to 0.6, then the tend becomes almost constant.

According to the results, a polynomial regression is defined in figure 4.6 with correlation factor of 96%. Indeed, a polynomial regression is a good relation to express the relation between (k_c/k_r) and backfill width ratio in case of soil friction angle of 33^0 .

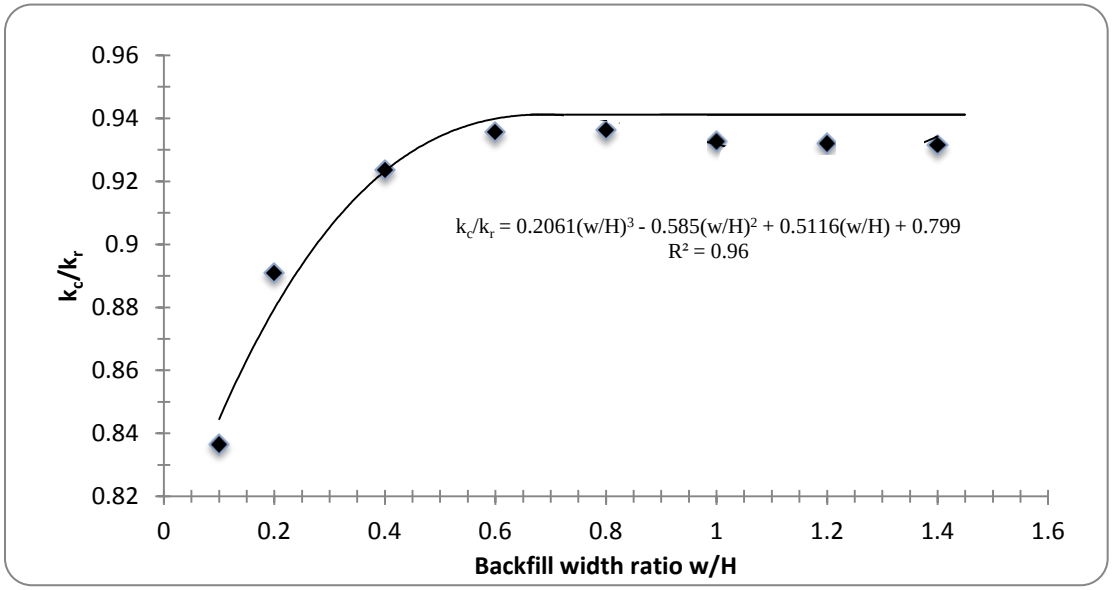

Figure 4.6: Relation between the backfill width ratio and k_c/k_r (in case of soil friction angle =33^0)

d. Earth Pressure Coefficient for Soil of $\phi=34^o$

Figure 4.7 highlights the relationship between ratios of (k_c/k_r) and backfill width ratios in case of soil friction angle = 34^0. The figure shows that the lateral earth pressure coefficient is increased as increasing the backfill width ratio up to (k_c/k_r) ratio of 0.6 then; it becomes almost constant. The maximum magnitude value for (k_c/k_r) ratio is 0.94 which is obviously less than that computed using the Rankine theory. Moreover, the results clearly show that a polynomial regression is fit to express the relation between the (k_c/k_r) ratio and the backfill width aspect ratio. The correlation factor exceeds 95% which clearly indicates a strong relation between backfill width ratio and lateral earth pressure coefficient for soil friction of 34^o.

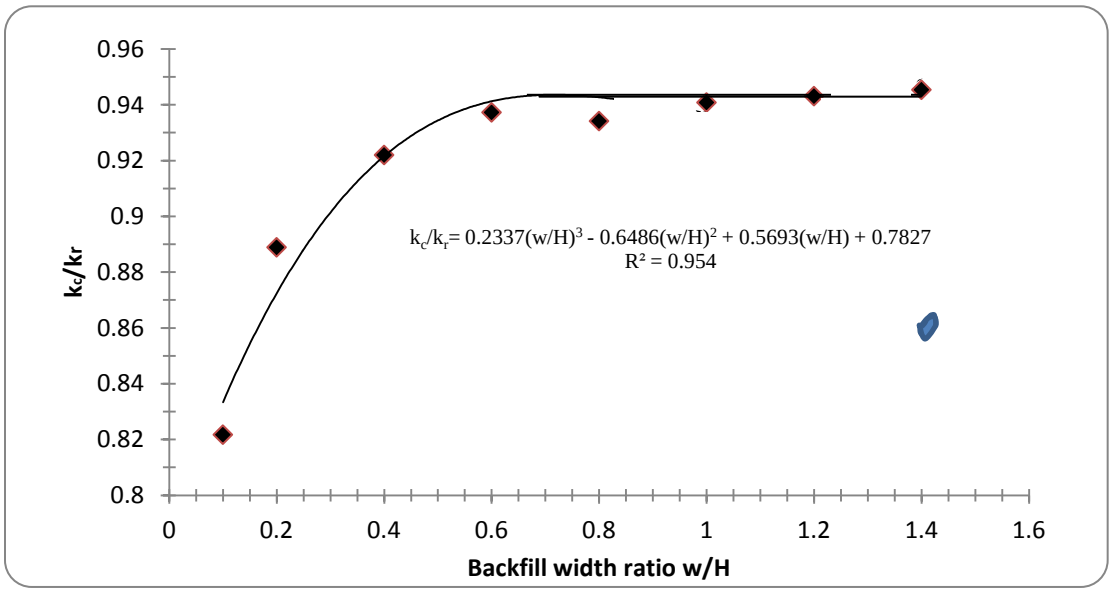

Figure 4.7: Relation between the backfill width ratio and k_c/k_r (in case of soil friction angle =34^0)

e. Earth Pressure Coefficient for Soil of $\phi = 35^0$

Figure 4.8 illustrates the relation between the backfill width ratio and lateral earth pressure coefficient ratio in case of soil friction angle = 35^0. The results clearly show that the normalized equivalent earth pressure coefficient is increased as the backfill width ratio increased and less than Rankine coefficient. Moreover, the variation between (k_c/k_r) ratios is decreased as the corresponding backfill width aspect ratio increased up to 0.6, then the tendency becomes almost constant.

Meanwhile, a polynomial regression is defined to describe the relationship between the (k_c/k_r) ratio and backfill width ratio with correlation factor of 97.8%. Indeed, this percent of correlation is very strong to express the relation between (k_c/k_r) ratio and backfill width in case of soil friction angle of 35^0

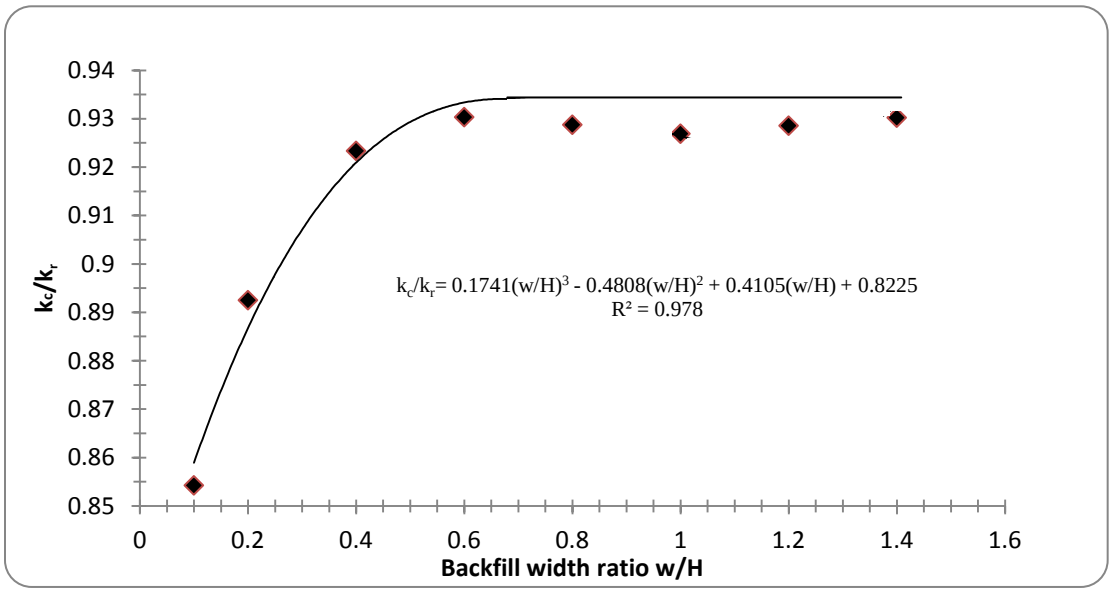

Figure 4.8: Relation between the backfill width ratio and k_c/k_r (in case of soil friction angle =35^0)

f. Earth Pressure Coefficient for Soil of $\phi = 36^0$

Figure 4.9 shows the relationship between the backfill width aspect ratio and the lateral earth pressure coefficient ratio in case of soil friction angle =36^0. The results indicate that the normalized equivalent earth pressure coefficients is increased as increasing the backfill width ratio and less than Rankine coefficient by 13% to 6% when the aspect ratio is changed from 0.1 to 1.4. The variation between (k_c/k_r) ratios is decreased gradually by increasing the backfill width ratio. Meanwhile, the aspect ratio has increasing tendency up to 0.6 then, becomes almost constant.

Furthermore, Figure 4.9 shows that a polynomial regression matches the results were obtained by plaxis model with correlation factor of 99%. Undeniably, a polynomial regression is a strong regression to express the relation between the equivalent earth pressure ratio and the backfill width aspect ratio for soil friction angle =36^0.

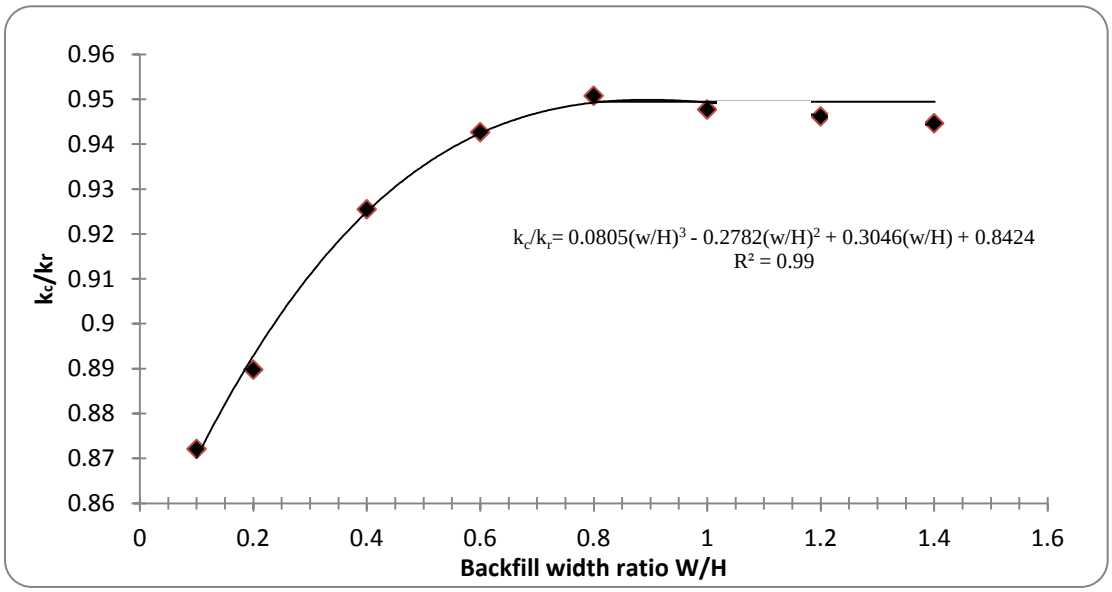

Figure 4.9: Relation between the backfill width ratio and k_c/k_r (in case of soil friction angle =36^0)

3. Summary of theoretical study

Figure 4.10 summarized the results obtained by the numerical modeling. Several charts are developed to show the relation between the backfill width ratio (w/H) and the equivalent lateral earth pressure coefficient ratios (k_c/k_r) for different values of soil friction angle ranging between 31^0-36^0. Based on these results, (k_c/k_r) ratio has obviously increasing tendency as (w/H) ratio increase. The magnitude value of (k_c/k_r) ratio is ranging between 0.82 to 0.87 at (w/H) ratio of 0.1, while (k_c/k_r) ratio is changed from 0.93 to 0.94 at (w/H) ratio of 1.4. The variation between the magnitude values of (k_c/k_r) ratio is decreased as the backfill width ratio increased while (k_c/k_r) becomes constant at (w/H) ratio more than 0.6.

Moreover, the results were obtained by numerical modeling have been averaged at each backfill width ratio for different values of soil friction angle ranging between 31^0-36^0 and a polynomial regression is defined to express the relation between (k_c/k_r) ratio and (w/H) ratio with correlation factor of 98.4 %.

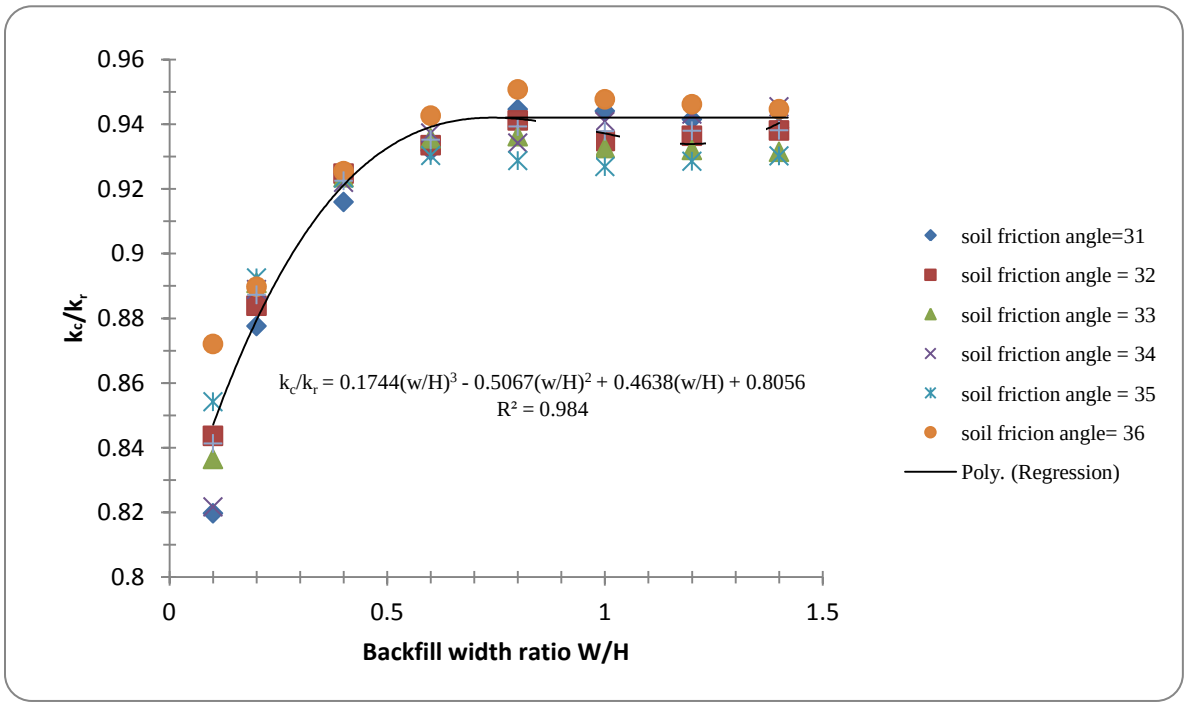

Figure 4.10: Relation between the backfill width ratio and k_c/k_r (in all case of soil friction angle)

4.2 Experimental Work

The experimental work has been conducted using a centrifugal model. This model aims at verifying and validating the obtained results from theoretical study. The centrifugal model was made of wooden material and has a box shape with dimensions of 1.2m height and 1.0m width. The long dimension which represents the backfill width is varied. Several models tests have been conducted to investigate the soil pressure behind the face of a retaining wall using Geo-kon device. Therefore, earth pressures were measured using vibrating wire device (pressure cell) in three different locations along wall face. Table 4.1 illustrates the distance where the pressure cell was placed. The pressure cell size was the governing factor to select the locations of measurement.

While carrying out the laboratory experiment, the main factor governing the lateral earth pressure has been taken into consideration, namely; width to height ratio (w/H). The backfill width ratio behind retaining wall (w/H) was varied between 0.2 to 1.2 with increment of 0.2, where 0.1 width ratio has not been conducted since the cell diameter is 22 cm, which could not be applied in case of 0.1 width ratio.

Table 4.1: The distance where pressure cell was set

No.	Position No.	Distance from the top of wall, (d/H) *
1.	Position #1	0.1
2.	Position #2	0.42
3.	Position #3	0.9

*: the ratio where the soil pressure were measured.

4.2.1 Backfill Material

Sandy soil has been used as a backfill behind the retaining wall. Samples of soil have been taken to identify the soil properties. The tests have been conducted namely, density and direct shear test. The results of the tests are summarized as follow, the soil density was 17.3 KN/m^3 and soil friction angle is 32^0.

4.2.2 Results of Experimental Work

The results of the experimental works are presented next taking into consideration the variation of earth pressure coefficient along the wall and the variation due to different backfill width ratios.

1.Normalized Earth Pressure Coefficient

Based on the experimental work, a number of charts were developed to show the normalized earth pressure coefficient profiles for active condition behind the wall face. These charts present the relation between the earth pressure coefficient and the depth where the soil pressure measured. The depth is presented as non-dimensional quantity (z/H) where, (z) is the depth of soil pressure measurement and (H) is the wall height. Similarly, the lateral earth pressure along the wall face is represented by a non-dimensional lateral earth pressure coefficient (k_c).

a.Normalized lateral earth pressure coefficient when (w/H) = 0.2

Figure 4.11 shows the relationship between the normalized lateral earth pressure coefficient (k_c) and depth to height ratios at (w/H) of 0.2. The results clearly show an increasing in lateral earth pressure coefficient with depth. Moreover, the results indicate that exponential regression is the best to express the relationship between the earth pressure coefficient (k_c) and depth ratio, where the correlation factor reaches to 95%.

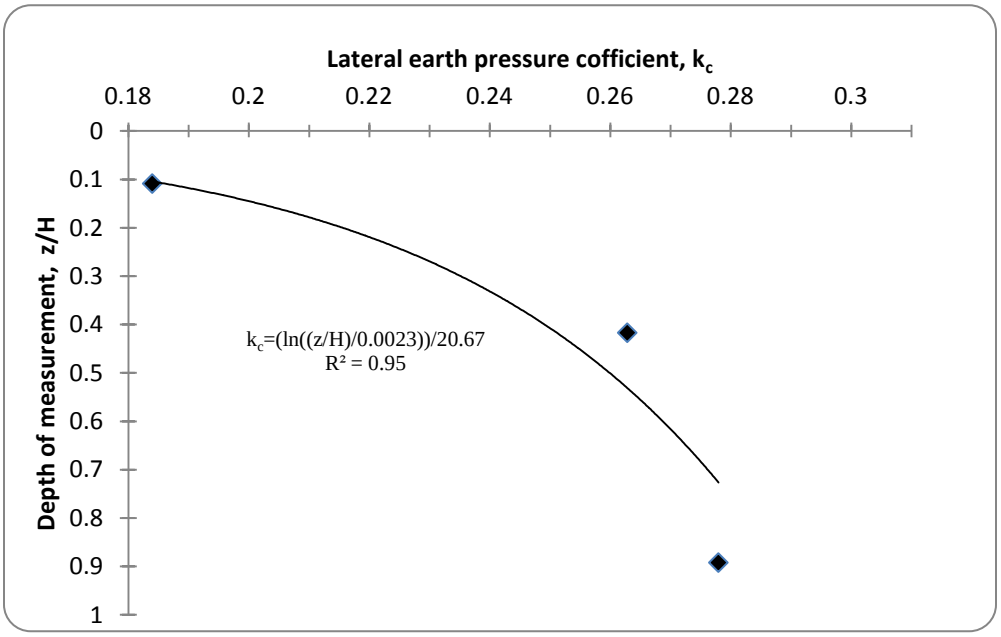

Figure 4.11: Lateral earth pressure coefficient behind the wall in case of (w/H) =0.2

b. Normalized lateral earth pressure coefficient when (w/H) =0.4

Figure 4.12 shows the relationship between the normalized lateral earth pressure coefficient (k_c) and (z/H) in case of w/H=0.4. The results also indicate an increasing of lateral earth pressure coefficient with depth ratio and exponential regression is defined with correlation of 96%.

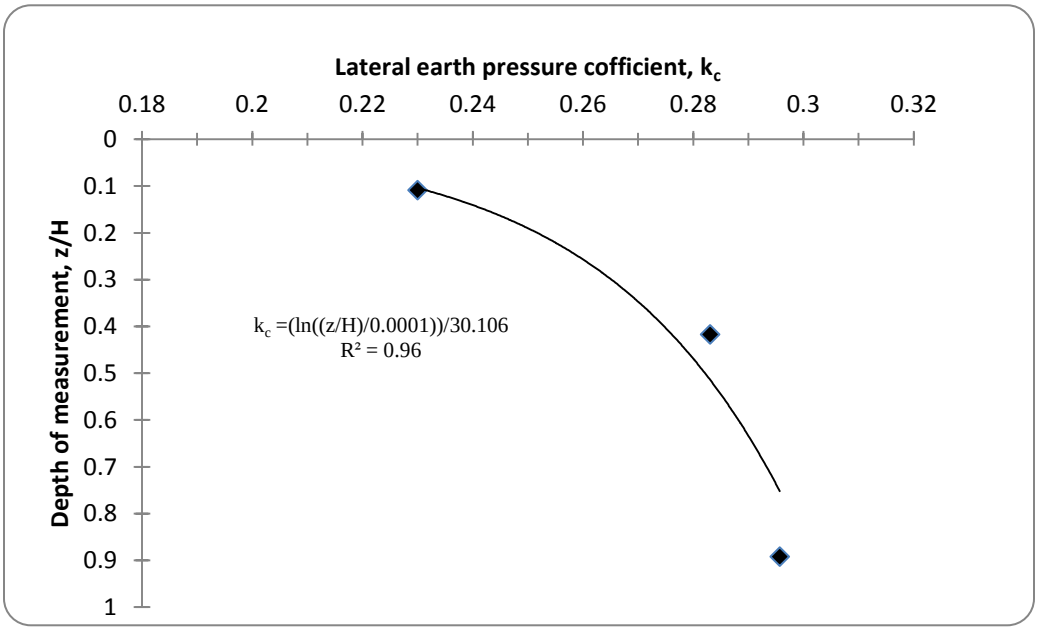

Figure 4.12: Lateral earth pressure coefficient behind the wall in case of (w/H) =0.4

c.Normalized lateral earth pressure coefficient when (w/H) = 0.6

Figure 4.13 shows the relationship between the normalized lateral earth pressure coefficient (k_c) and depth ratios when w/H=0.6. However, the results point out an increasing tendency for lateral earth pressure coefficient with depth ratio which is similar to the previous charts, the variation between magnitude values of k_c almost becomes small with depth ratio increasing which are clearly shown at z/H of 0.42 and 0.9. A exponential regression is also defined with correlation factor of 98%.

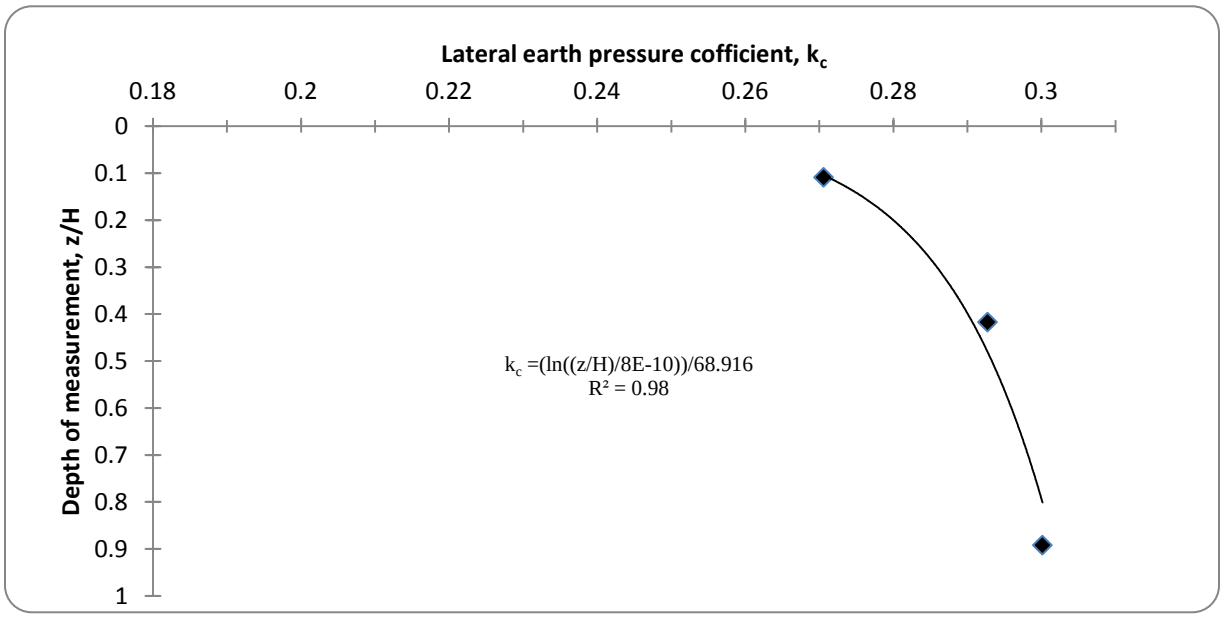

Figure 4.13: Lateral earth pressure coefficient behind the wall in case of (w/H) =0.6

d. Normalized lateral earth pressure coefficient when (w/H) = 0.8

Figure 4.14 illustrates the relationship between the normalized lateral earth pressure coefficient (k_c) and depth ratio when w/H=0.8. Results indicate that as w/H increase, the change of k_c with depth ratio become negligible. Furthermore, the results indicate that a exponential regression is the best to express the relationship between earth pressure coefficient (**k_c**) and depth ratio, where the correlation factor reaches to 80 %.

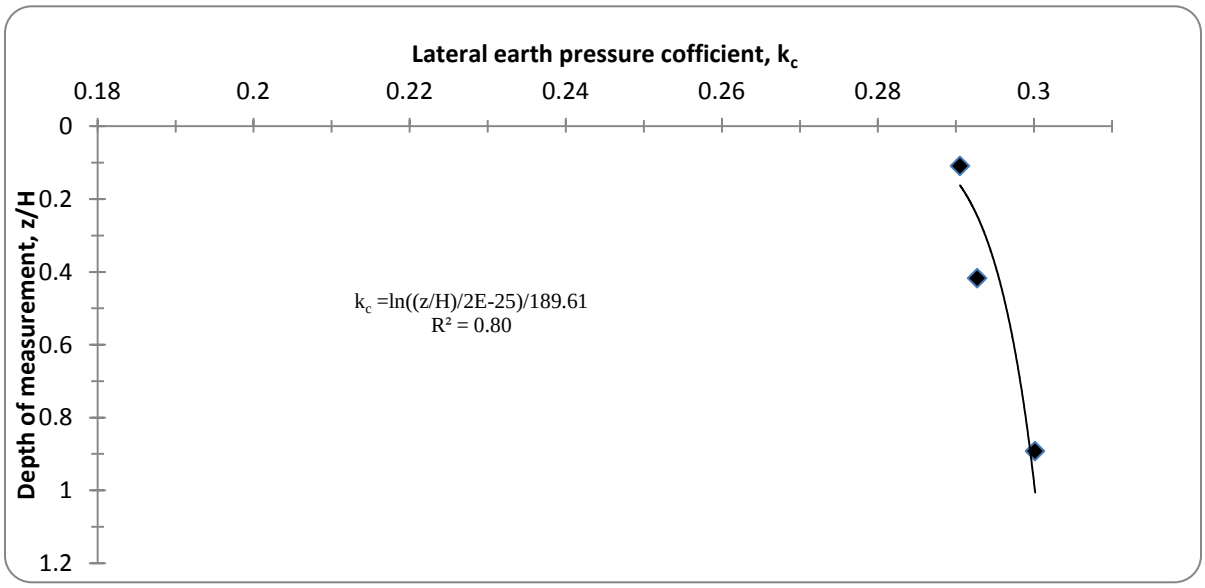

Figure 4.14: Lateral earth pressure coefficient behind the wall in case of (w/H) =0.8

e.Normalized lateral earth pressure coefficient when (w/H) = 1

Figure 4.15 shows the relation between the normalized lateral earth pressure coefficient (k_c) and depth ratio when w/H=1. The results indicate that a exponential regression is the best to express the relationship between earth pressure coefficient (k_c) and depth ratio with correlation factor of 74%.

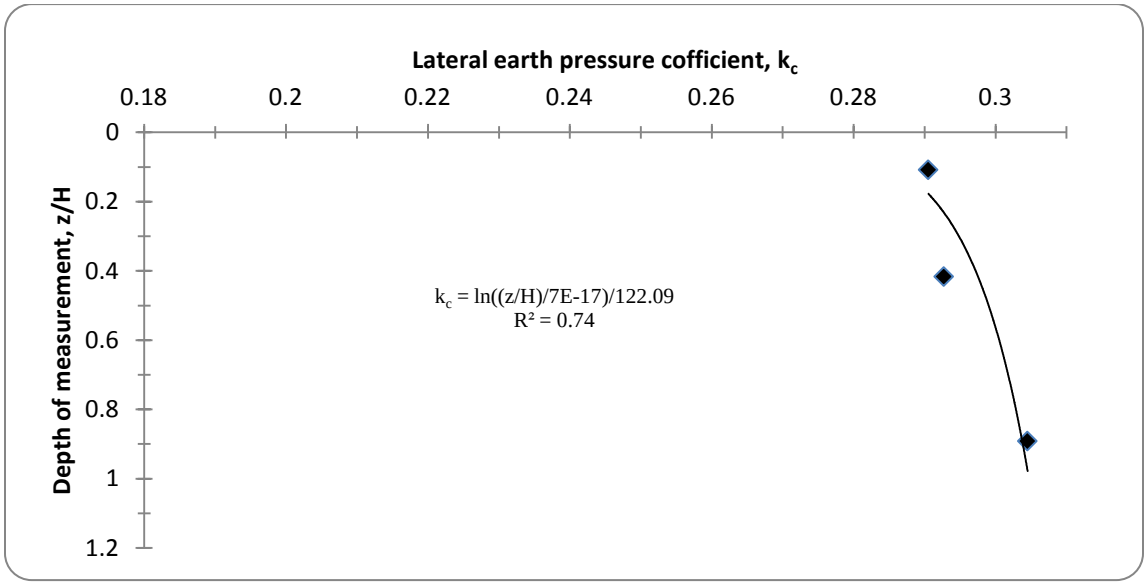

Figure 4.15: Lateral earth pressure coefficient behind the wall in case of (w/H) =1

f. Normalized lateral earth pressure coefficient when (w/H) = 1.2

Figure 4.16 shows the relationship between the normalized lateral earth pressure coefficient (k_c) and depth ratio when w/H= 1.2. It has a result which is similar to Figure 4.15.

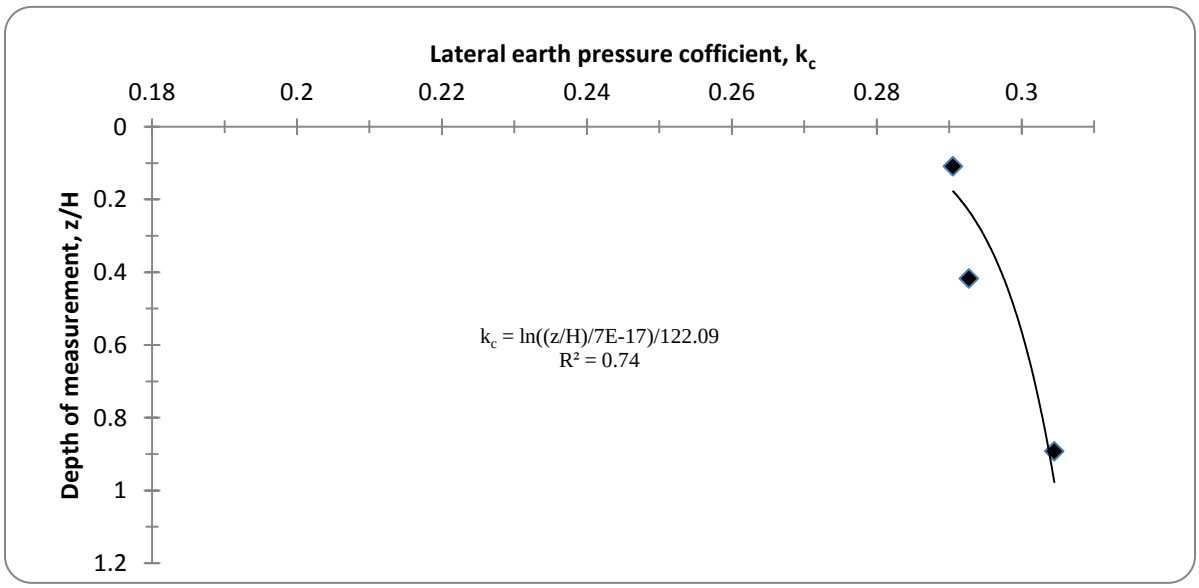

Figure 4.16: Lateral earth pressure coefficient behind the wall in case of (w/H) =1.2

2. Effect of fill-space geometry on active earth pressures

Effect of fill-space dimensions were taken into consideration in this study. A number of charts were developed to show the relationship between lateral earth pressure (k_c) and the backfill width ratio (w/H). These charts target each point mentioned in Table 4.1 individually.

a. Effect of fill-space geometry on active earth pressure at depth of d/H=0.1

Figure 4.17 shows the relationship between the backfill width ratio (w/H) and the lateral earth pressure coefficient (k_c) at depth ratio (d/H= 0.1). Results indicates that lateral earth pressure coefficient (k_c) is increasing with increasing the backfill width ratio (w/H).

A polynomial regression is defined to express the relationship between (k_c) and (w/H) ratio with correlation factor of 99%.

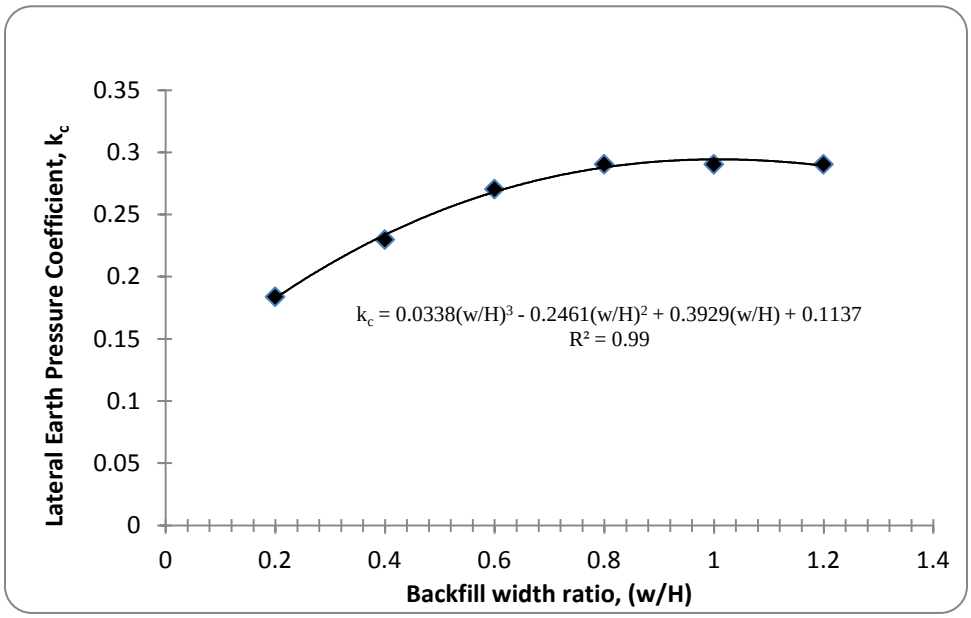

Figure 4.17: The relation between equivalent earth pressure coefficient and backfill width ratio at depth of (d/H=0.1)

b. Effect of fill-space geometry on active earth pressures at depth of d/H=0.42

Figure 4.18 shows the relation between the backfill width ratio (w/H) and the lateral earth pressure coefficient (k_c) at depth ratio (d/H= 0.42). However, the results indicate that the (k_c) is increased with increasing of backfill width ratio (w/H) up to 0.6.

A polynomial regression is defined to express the relationship between (k_c) and (w/H) ratio with correlation factor of 99%.

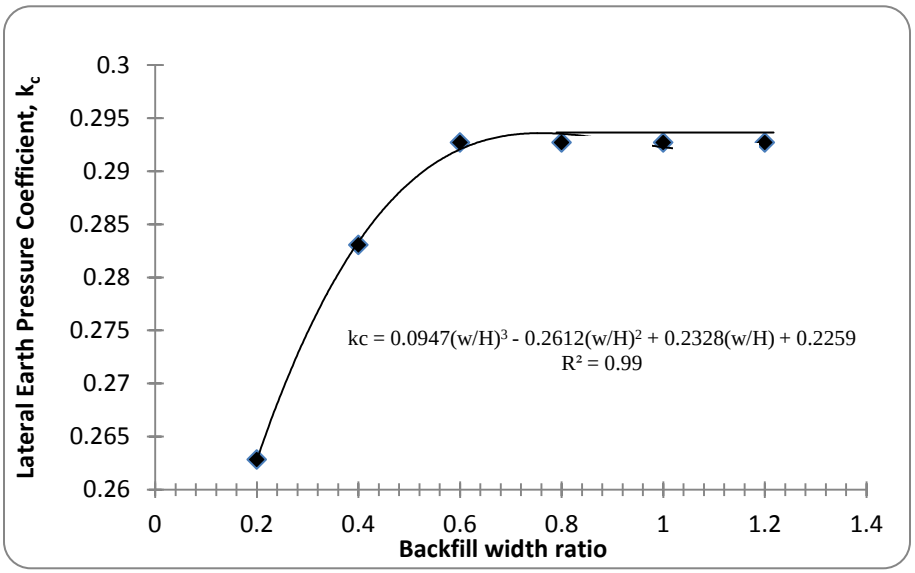

Figure 4.18: The relation between equivalent earth pressure coefficient and backfill width ratio at depth of d/H=0.42

c. Effect of fill-space geometry on active earth pressures at depth of d/H=0.9

Figure 4.19 shows that relation between backfill width to height ratio (w/H) and lateral earth pressure coefficient at depth of d/H=0.9. A polynomial regression is also defined to express the relationship between (k_c) and (w/H) ratio with correlation factor of 97.5%.

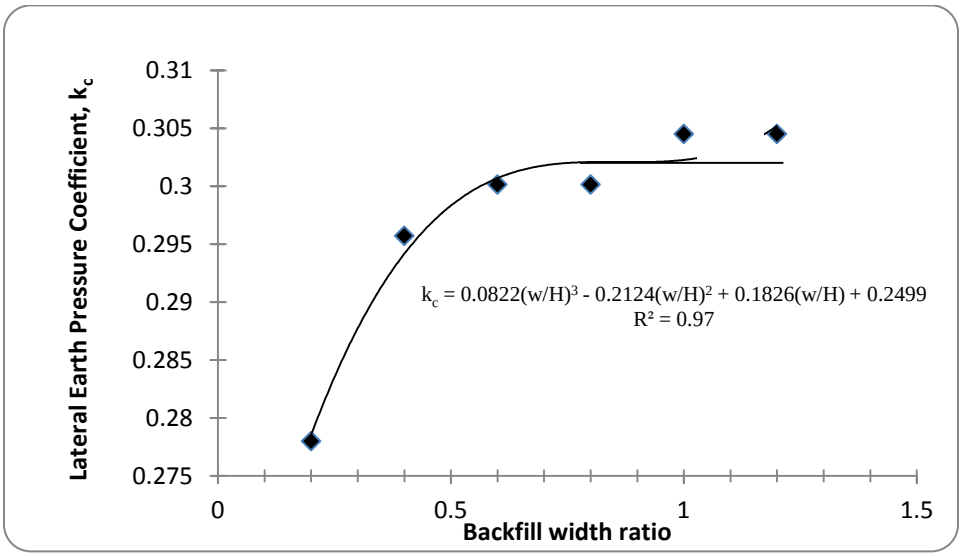

Figure 4.19: The relation between equivalent earth pressure coefficient and backfill width ratio at d/H=0.9

3. Summary of experimental work results

Figure (4.20) shows the relation between the equivalent earth pressure coefficient ratio and backfill width ratio and a polynomial regression was defined to express this relationship with correlation factor of 99%. The width is presented as non-dimensional quantity (w/H) where (w) is the width of backfill and (H) is the wall height. Similarly, the lateral earth pressure along the wall face is represented by a non-dimensional lateral earth pressure coefficient (k_c/k_r), where k_c is the calculated coefficient through the experimental work and k_r is related to Rankine coefficient which could be obtained by $k_r = tan^2\left(45 - \frac{\emptyset}{2}\right)$.

However, the results show that (k_c/k_r) ratio is increased with increasing the backfill width ratio, the ratio of (k_c/k_r) considerably becomes constant at (w/H) ratio of more than 0.6.

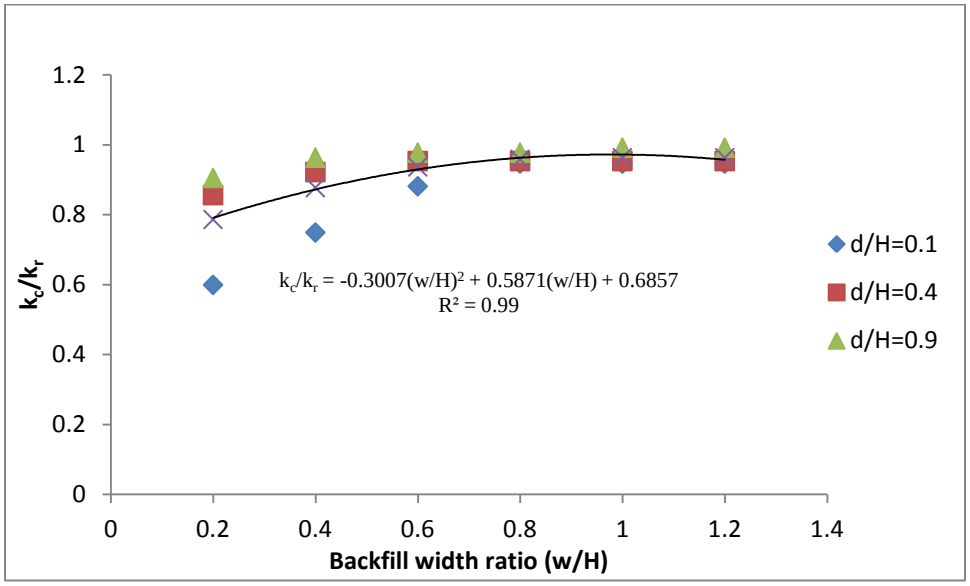

Figure 4.20: Relation between the backfill width ratio and the equivalent lateral earth pressure ratio (k_c/k_r)

4.3 Comparison between Results

Figure 4.21 shows a comparison between the results of experimental work, theoretical study and previous studies. These results are presented as (k_c/k_r) ratio versus backfill width ratio (w/H).

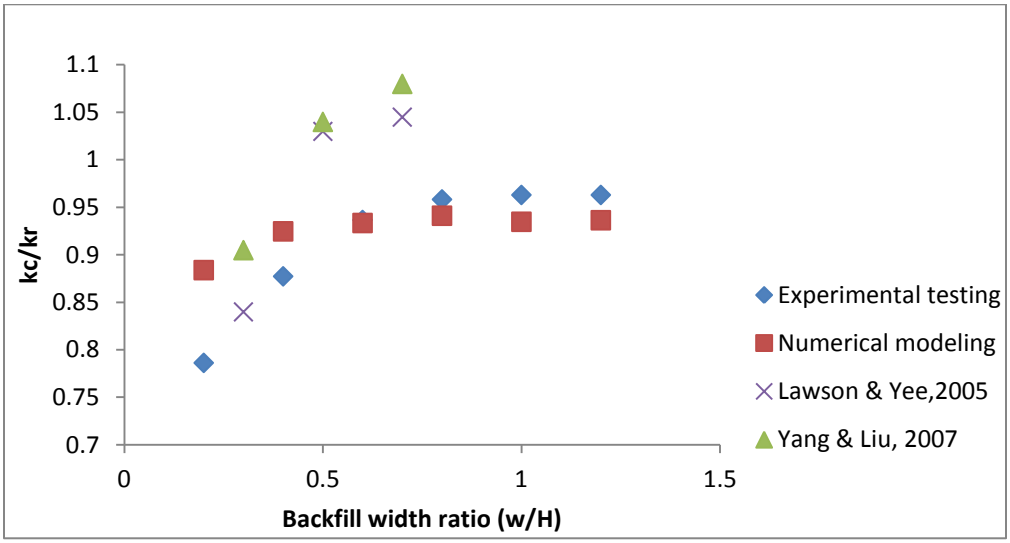

Figure 4.21: Normalized equivalent earth pressure coefficients for active case

Based on Figure (4.21), decrease of earth pressures becomes prominent as the width of the wall becomes less. Besides, the results obviously indicate that (k_c/k_r) ratios are less than Rankine coefficient according to experimental and theoretical study, but the previous studies regarding the Lawson & Yee,2005 and Yang & Liu,2007 show that the ratio k_c is less than Rankine coefficient for (w/H) less than 0.5. This implies that the boundary constraint plays an important role when the backfill behind retaining wall is limited. In addition, Rankine theory was derived assuming the failure plane is linear, but the actual plane is curved as shown in Figure 4.22.

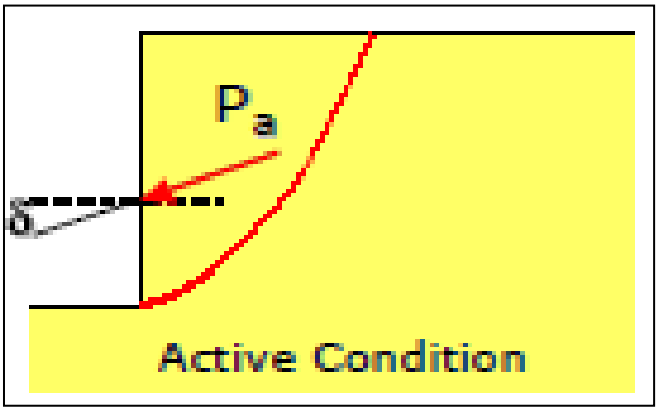

Figure 4.22: Actual failure plan for active condition (Kame et al, 2010**)**

The results of both numerical and experimental studies indicates that the (k_c/k_r) become constant when backfill width ratio (w/H) is more than 0.6, but (w/H) ratio become almost

constant at more than 0.5 for previous studies . The results of this research give a good agreement with Rankine assumption for failure at angle $45 + \frac{\emptyset}{2}$ as shown in Figure 4.23. Table 4.2 illustrates the (w/H) ratio where the failure plane is occurred based on Rankine theory and numerical modeling.

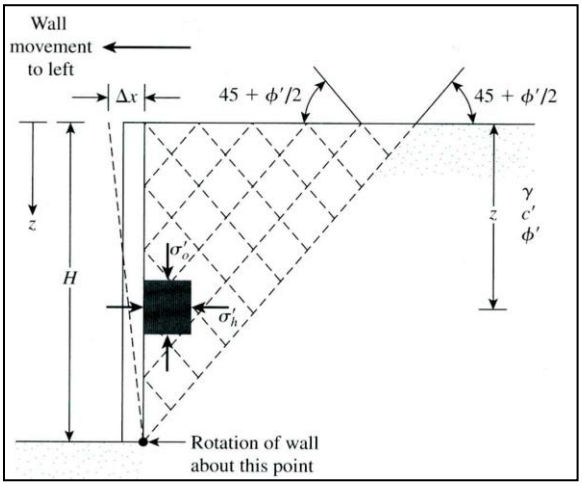

Figure 4.23: Rankine's active pressure (Das, 2011**)**

Table 4.2: The distance of failure plane from wall face for different values of soil friction angle

Friction angle (Ø)	(w/H) Rankine Theory	(w/H) Theoretical study
31	0.57	0.65
32	0.55	0.6
33	0.54	0.6
34	0.53	0.6
35	0.52	0.6
36	0.51	0.6

4.4 Convergence between experimental work and theoretical study

In this research, the experimental work was conducted for different backfill width ratios in case of soil friction angle 32^0. Meanwhile, the theoretical study was performed at different values of soil friction angle ranging between 31^0 to 36^0. Based on both results of experimental work and theoretical study, Figure 4.24 shows the developed chats at different values of soil friction angle to foresee the results experimentally. These charts indicates that the effect of soil friction angle on (k_c/k_r) ratio is negligible.

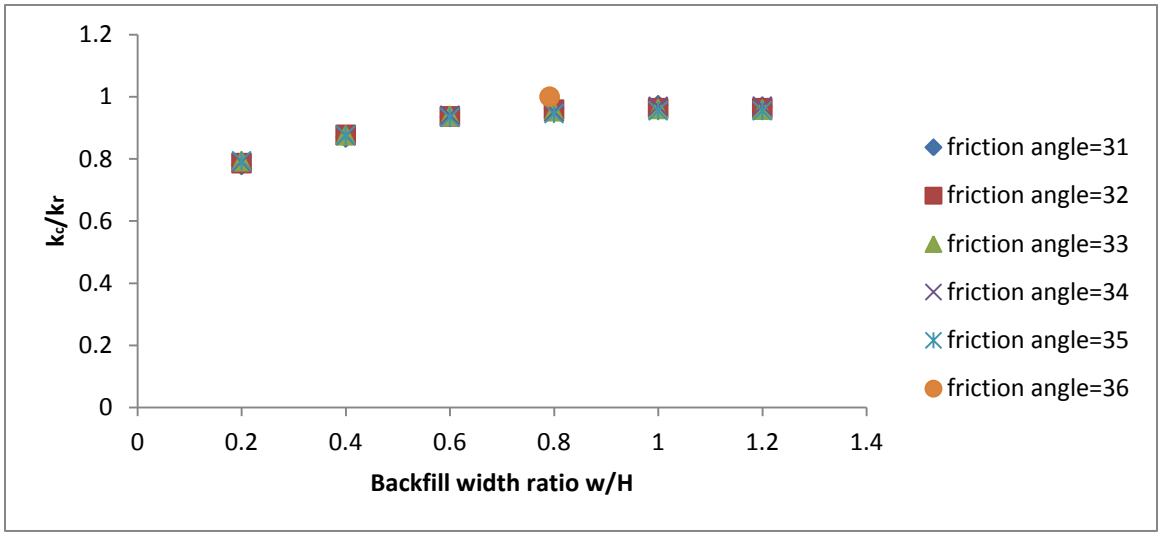

Figure 4.24: Predicted of k_c/k_r for different friction angles based on experimental and theoretical results.

Chapter 5
Conclusions and Recommendations

5.1 Conclusions

This study investigated active earth pressures on rigid retaining walls in case of narrow backfill. Both of theoretical study and experimental work have been carried out. The theoretical study was conducted using numerical modeling (plaxis software program) and the experimental work was implemented to verify and validate the results obtained by the theoretical study using centrifugal model and Geo-kon device to measure the soil pressure.

From both theoretical study and experimental work that were performed in this research, the conclusion can be drawn as following

- Theoretical study was carried out at different values of soil friction angle ranging between 31^0-36^0. Based on these results, (k_c/k_r) ratio has obviously increasing tendency by increasing (w/H) ratio. The results show that the lateral earth pressure coefficient at active condition is less than rankine coefficient since; the magnitude value of (k_c/k_r) ratio is ranging between 0.82 to 0.87 at (w/H) ratio of 0.1, while (k_c/k_r) ratio is changed from 0.93 to 0.94 at (w/H) ratio of 1.4. The variation between the magnitude values of (k_c/k_r) ratio is decreased as the backfill width ratio increased where (k_c/k_r) considerably becomes constant at (w/H) ratio more than 0.6.
- The experimental work was performed for soil friction angle $\emptyset = 32^0$ and different backfill width ratios ranging between 0.2 to 1.2 with increment of 0.2. The results shown that the lateral earth pressure coefficient is increased with depth and backfill width ratio of (w/H) and less than rankine coefficient. Furthermore, (k_c/k_r) becomes constant at (w/H) ratio of 0.6.
- Convergences between the experimental work and theoretical study and number of charts have been developed for different soil friction angles.

- The results indicated that the effect of soil friction angle is negligible through presentation the relationship between the backfill width ratio (w/H) and the lateral earth pressure coefficient ratio (k_c/k_r)

5.2 Recommendations

In the present study, the scope was only focused on the earth pressures of narrow retaining walls. In the future study, it is recommended to study the effect of seismic loadings and surcharge.

References

- Bowel, J. (1988). *Foundation Analysis and Design* (4th ed.). MCGRAW.
- Brinkgreve, R. B. (2002). *Plaxis Manual.* Netherland: Delf University of Technology.
- Das, B. (2011). *Principles of Foundation Engineering.* Pennsylvania: Christopher M. Shortt.
- Fan, C., & Fang, Y. (2010). Numerical Solution of active earth pressures on rigid retaining walls built near rock faces. *ELSEVIER* .
- Frydman, S., & Keissar, I. (1987). Earth pressure on retaining walls near rock faces. *Journal of Geotechnical Engineering, ASCE , Vol. 113, No. 6,* 586-599.
- Goh, A. (1993). Behavior of Cantilever Retaining Walls. *Journal of Geotechnical Engineering , Vol. 119, No. 11*, 1751-1770.
- Kame, G. S., Dewaiker, D. M., & Choudhury, D. (2010). Active Thrust on a Vertical Retaining Wall with Cohesionless Backfill. *EJGE , 15*, 1848-1862.
- Lawson, C., & Yee, T. (2005). Reinforced soil retaining walls with constrained reinforced fill zones. *Geo-Frontiers.* ASCE Geo-Institute Conference.
- Leshchinsky, D., Hu, Y., & Han, J. (2003). Design implications of limited reinforced zone space in SRW's. *The 17th GRI Conference on Hot Topics in Geosynthetics IV.* Las Vegas: Nevada.
- Motta, E. (1994). Generalized Coulomb Active Earth Pressure for Distanced Surcharge. *Journal of Geotechnical Engineering , Vol.120, No.6,* 1072-1079.
- Spangler, M., & Handy, R. (1982). *Soil Engineering* (4th ed.). New York: Harper and Row.
- Take, W., & Valsagkar, A. (2001). Earth pressure on unyielding retaining walls of narrow backfill width. *Canadian Geotechnical Journal* , pp. 1220-1230.
- Wahab, R. (2008). *Design of Retaining Wall by Finite Element Using Plaxis.* Malaysia: University of Technology.
- Yang, K.-H., & Liu, C.-N. (2007, August). Finite element analysis of earth pressure for narrow retaining walls. *Journal of GeoEngineering , 2* (2), pp. 43-52.

Appendix

Photos Show the Work in the Laboratory